Computers and Chemical Engineering 191 (2024) 108836

Contents lists available at ScienceDirect

Computers and Chemical Engineering

journal homepage: www.elsevier.com/locate/compchemeng

Optimization of sustainable supply chain for bio-based isopropanol production from sugar beet using techno-economic and life cycle analysis

Ching-Mei Wen, Marianthi Ierapetritou *

Department of Chemical & Bio-molecular Engineering, University of Delaware, Newark, DE, United States

ARTICLE INFO

Keywords:
Techno-economics analysis
Life cycle assessment
Sugar Beet-to-Isopropanol
Optimization
Supply chain
Geographical Information System

ABSTRACT

This study examines the techno-economic and life cycle analysis of bio-based isopropanol (IPA) production from sugar beet, utilizing a Geographical Information System (GIS)-enabled framework. By focusing on the innovative IPA production technology, the research demonstrates the economic and environmental feasibility of converting first-generation biomass into sustainable chemicals through the optimization of the Sugar Beet-to-Isopropanol supply chain. Findings highlight a cost-optimal production capacity of 55,800 mt/year with significant potential for reducing emissions and operational costs. The production cost of bio-IPA is potentially 70 % less than the fossil-derived IPA price. Additionally, the potential profits from bio-based IPA are estimated to be nearly double the market price of its primary raw material, sugar, demonstrating the economic feasibility of converting the first-generation biomass for sustainable IPA production. The study also explores the impact of facility clustering on transportation emissions and costs, revealing strategic approaches to expanding plant capacities in response to increasing demand. This research provides insights for designing sustainable industrial practices using first-generation biomass in the chemical industry.

1. Introduction

Striving to find eco-friendly alternatives to traditional petrochemical products, bio-based chemicals have emerged as a promising solution (Fiorentino et al., 2019). These chemicals are sourced from renewable biological materials such as plants, algae, and specific waste, providing a greener option to similar products made from petrochemicals (Fiorentino et al., 2019; Mohanty et al., 2002; Yue et al., 2014). Unlike finite fossil fuels, biomass operates on a cyclical paradigm, sequestering CO_2 during growth and making the chemicals produced from it essentially carbon neutral (Chung et al., 2023; Lim et al., 2023). Recent advances in biotechnology, genetic engineering, and chemical processes have improved the efficiency of biomass conversion to chemicals and increased its commercial viability (Gavrilescu and Chisti, 2005; Wyman and Goodman, 1993). While extensive literature addresses the utilization of second to fourth-generation biomass (You et al., 2012; Sharma et al., 2013; Ng and Maravelias, 2016; An et al., 2011; O'Neill et al., 2022), focusing on the economic and environmental impacts of existing and proposed technologies, the first-generation biomass, extracted from food sources like C6 sugars, is noteworthy (Lee and Lavoie, 2013; Miret et al., 2016). Despite its prices are higher than those of second-generation biomass, it is still produced on a global scale of 170–180 million tons (Lopes, 2015), making first-generation biomass a predominant and the most available choice in the bio-based industry. In countries like Brazil, sugar-derived bioethanol has proven to be economically viable, highlighting the potential of first-generation biomass (Osman et al., 2021).

The production of sugars, including glucose, fructose, and sucrose, represents a significant segment of the U.S. agricultural industry, especially within its robust sugarcane and sugar beet sectors (Eggleston and Lima, 2015; Duraisam et al., 2017). In recent years, there has been a surge in efforts to utilize these sugars for the production of bio-based chemicals (Liew et al., 2022; Charubin and Papoutsakis, 2019; Foster et al., 2021; Zhang et al., 2011; Swidah et al., 2015). Focusing on this realm, one prime example is the synthesis of bio-based isopropanol (IPA) (Liew et al., 2022; Charubin and Papoutsakis, 2019; Foster et al., 2021; Zhang et al., 2011; Swidah et al., 2015). Genetically engineered strains of *E. coli* have been modified to optimize IPA yield resulting in a carbon-negative production (Liew et al., 2022). Similarly, Clostridium species, especially *C. acetobutylicum* and *C. ljungdahli*, have been employed due to their unique metabolic pathways, specifically the potential of CO_2 utilization via the Wood-Ljungdahhl pathway, as outlined by (Charubin and Papoutsakis, 2019; Foster et al., 2021). Beyond these,

* Corresponding author.
E-mail address: mgi@udel.edu (M. Ierapetritou).

https://doi.org/10.1016/j.compchemeng.2024.108836
Received 22 January 2024; Received in revised form 18 June 2024; Accepted 11 August 2024
Available online 22 August 2024
0098-1354/© 2024 Elsevier Ltd. All rights are reserved, including those for text and data mining, AI training, and similar technologies.

Nomenclature

Sets/Indices

I	Set of sugar beet supply counties index by i
J	Set of sugar plants indexed by j
K	Set of IPA production sites indexed by k

Parameters

BS	The required supply of sugar beet (biomass) for producing every 141,360 mt of IPA, mt/yr
SS	The required supply of sugar for producing every 141,360 mt of IPA, mt/yr
α	The weight loss of sugar beet covert to sugar
β	The weight ratio of sugar and carbon dioxide in the stoichiometric equation
θ	Parameter for investment capital cost
b_i	The sugar beet availability in county i
c_i	The sugar beet unit cost ($/mt) in county i
s	Auxiliary parameters used for changing the target IPA production capacity
$\zeta^{S,min}_{l=small}$	The minimum capacity of the sugar plant in the level of small ($l = small$)
$\zeta^{S,max}_{l=small}$	The maximum capacity of the sugar plant in the level of small ($l = small$)
$\zeta^{S,min}_{l=medium}$	The minimum capacity of the sugar plant in the level of small ($l = medium$)
$\zeta^{S,max}_{l=medium}$	The maximum capacity of the sugar plant in the level of small ($l = medium$)
$\zeta^{S,min}_{l=large}$	The minimum capacity of the sugar plant in the level of small ($l = large$)
$\zeta^{S,max}_{l=large}$	The maximum capacity of the sugar plant in the level of small ($l = large$)
$\zeta^{A,min}_{l=small}$	The minimum capacity of the bio-IPA plant in the level of small ($l = small$)
$\zeta^{A,max}_{l=small}$	The maximum capacity of the bio-IPA plant in the level of small ($l = small$)
$\zeta^{A,min}_{l=medium}$	The minimum capacity of the bio-IPA plant in the level of small ($l = medium$)
$\zeta^{A,max}_{l=medium}$	The maximum capacity of the bio-IPA plant in the level of small ($l = medium$)
$\zeta^{A,min}_{l=large}$	The minimum capacity of the bio-IPA plant in the level of small ($l = large$)
$\zeta^{A,max}_{l=large}$	The maximum capacity of the bio-IPA plant in the level of small ($l = large$)
$C^{FS,Tf}$	The transportation fixed cost for sugar beet ($/mt)
$C^{SA,Tf}$	The transportation fixed cost for sugar ($/mt)
$C^{FS,Tv}$	The transportation variable cost for sugar beet($/mt -km) ($/mt -km)
$C^{SA,Tv}$	The transportation variable cost for sugar ($/mt -km)
d_{ij}	The shortest distance for sugar beet supply county (i) to sugar plant (j) in km
d_{jk}	The shortest distance for sugar plant (j) to IPA plant (k) in km
$C^{Sc,v}_l$	The variable capital cost for producing sugar at level l ($)
$C^{Sc,f}_l$	The fixed capital cost for producing sugar at level l ($/mt)
$C^{So,unit}$	The unit operation cost for producing sugar ($/mt)
$C^{Ac,v}_l$	The variable capital cost for producing bio-IPA at level l ($)
$C^{Ac,f}_l$	The fixed capital cost for producing bio-IPA at level l ($/mt)
$C^{Ao,unit}$	The unit operation cost for producing sugar ($/mt)
$C^{G,v}_l$	The fixed cost of capturing CO_2
$C^{G,f}_l$	The variable cost of capturing CO_2
$\lambda^{sugar\ beet}$	GWP100 characterization factor of sugar beet harvest (CO_2-eq /mt)
λ^{truck}	GWP100 characterization factor of truck transportation (CO_2-eq /mt-km)
λ^{sugar}	GWP100 characterization factor of beet sugar production process (CO_2-eq /mt)
λ^{IPA}_l	GWP100 characterization factor of bio-IPA production process (CO_2-eq /mt)
$\lambda^{carbon\ capture}$	GWP100 characterization factor of capturing CO_2 (CO_2-eq /mt)
$D^{CO_2}_k$	The available amount of CO_2 in site k

Binary variables

$e^S_{j,l}$	0–1 variable for the selection of sugar plant j at level l
$e^A_{k,l}$	0–1 variable for the selection of IPA factory site k at level l
e^F_i	0–1 variable for the selection of sugar beet supply county i
e^S_j	0–1 variable for the selection of sugar plant j
e^A_k	0–1 variable for the selection of IPA factory site k

Decision variables

$flow^{FS}_{i,j}$	The sugar beet flow received by sugar plant j from sugar beet supply county i.
$flow^{SA}_{j,k}$	The sugar flow received by bio-IPA plant k from sugar production plant j.
$s^S_{j,l}$	The production amount of sugar in sugar plant j with level indexed by l
$s^A_{k,l}$	The production amount of bio-IPA in IPA factory k with level indexed by l

Nonnegative continuous variables

C^F	The cost of sugar beet purchase
C^T	The cost of transportation
C^S	The cost of sugar production process
C^G	The cost of CO_2 capture process
C^A	The cost of bio-IPA production process
C^{Tf}	The net cost of variable transportation
C^{Tv}	The net cost of fixed transportation
C^{So}	The operation cost of sugar plant
C^{Sc}	The capital cost of sugar plant
C^{Ao}	The operation cost of bio-IPA plant
C^{Ac}	The capital cost of bio-IPA plant
G^F	The net emission from sugar beet harvest with GWP100 indicator
G^T	The net emission from transportation with GWP100 indicator
G^S	The net emission from sugar production with GWP100 indicator
G^G	The net emission from CO_2 capture process with GWP100 indicator
G^A	The net emission from bio-IPA production with GWP100 indicator

there has been practice using yeast strains, like Saccharomyces cerevisiae, engineered for IPA production (Zhang et al., 2011), further expanding the range of bio-based approaches. These engineered microorganisms demonstrate the economic and environmental potential of converting simple sugars to IPA. Reflecting on a national scale, Minnesota, the largest producer of sugar in the U.S. might be a significant contributor to the industry, with sugar beet production alone supplying over 33 % of the nation's sugar (Bangsund et al., 2004), highlighting the state's potential in sustainable IPA production using sugar beets.

Although the concept of converting one commodity to another holds potential (Cheng et al., 2019; Fenila and Shastri, 2020), there are still a number of challenges to overcome. One of the major obstacles is the complexity of the economics involved, particularly concerning feedstock prices which play a critical role in the process. For example, in 2012, raw sugar was priced near $0.44 per kilogram (Lee and Lavoie, 2013). The cost of producing ethanol from sugar was estimated at $0.38 to $0.44 per kilogram, which was nearly equivalent to the market price of sugar. After considering additional operating expenses, these production costs would likely meet or exceed the potential revenue from selling ethanol (with the ethanol market price at roughly $0.86 per kilogram (Lee and Lavoie, 2013)), thereby reducing or nullifying profits. As a result, it may have been more economically efficient to sell the sugar directly rather than converting it into ethanol. Meanwhile, the environmental impact is a major concern as well. The reliance on fossil fuels, particularly in transportation, contributes to increased greenhouse gas (GHG) emissions. Therefore, prioritizing restructuring of the supply chain for sustainable alternatives has become crucial (Jafari-Nodoushan et al., 2024; Perez et al., 2022). To balance economic and environmental objectives, comprehensive optimization of the supply chain is required, which includes careful decision-making when it comes to biomass sourcing, site selections, biorefinery capacities, and more. Our study takes a comprehensive analysis of the three-tier Sugar Beet-to-Isopropanol supply chain as Fig. 1 shown. The study emphasizes a Techno-Economic Analysis (TEA) and Life Cycle Assessment (LCA) to provide an in-depth understanding of the process. The main finding is that converting first-generation biomass to isopropanol can be both economically and environmentally beneficial.

The application of geospatial tools, notably the Geographical Information System (GIS) (Burrough et al., 2015), plays a crucial role in conducting precise agro-resource assessments, optimizing biomass logistics, and informing plant scale design decisions. Additionally, the incorporation of TEA and LCA methodologies facilitates a comprehensive understanding of the potential impacts of biotechnological processes on various economic and environmental parameters. In line with the above discussion, the work analyzed the potential applications of GIS, spatial TEA, and LCA in the sustainable planning of first-generation biomass-based bioenergy programs. Through an examination of Minnesota's geospatial data, 25 counties for the supply of sugar beet were identified, along with 5 major sugar production facilities. In a move towards efficiency, potential locations for IPA plants have been selected in proximity to 19 existing ethanol plants, capitalizing on current infrastructure, available resources, and established regulatory pathways. Insights regarding biomass yields, supply dynamics, and cost structures were derived from this geospatial information and further enriched by techno-economic and life cycle assessments. This paper aims to fill this gap by testing the applicability of the developing technology with real-world spatial differences and identifying challenges and potentials for the design of sustainability in biomass-based IPA supply chains. The study includes a discussion on the role of GIS in biomass resource assessment, biomass logistics planning, and bioenergy plant scale design. The remainder of this paper is organized as follows: The methodology section introduces the spatial information of the sugar beet-to-IPA supply chain system, the TEA and LCA estimation of the technologies, and the proposed formulation of cases: (i) for determining the maximum and minimum (feasible) IPA production capacities, Mixed Integer Linear Programming (MILP) is solved; (ii) Multi-objective Mixed Integer Linear Programming (MILP) is applied for assessing economic and environmental performance; (iii) the MILP is solved multiple times with the ϵ-constraint method (Pappas et al., 2021; Lopes et al., 2020) in varying of IPA capacity to generate the Pareto set of optimal solutions in the objective function space of the multi-objective optimization problem, and its constraints. In the result section, the systematic analysis of the optimal design and planning models is based on the proposed model. Finally, conclusions and directions for future studies are provided.

2. Methodology

The study addresses a supply chain designing problem in large-scale bio-IPA production (accounting for >7 % of the U.S. production of isopropanol (American Chemistry, Statista 2020)) by formulating it as a multi-objective Mixed Integer Linear Programming (MILP) problem (for case (ii), optimizing the economic and environmental performance). This approach integrates GIS applications for analyzing the biomass to bio-IPA supply chain, focusing on optimizing mass and energy flows, economies of scale, and site-specific emission and economic conditions.

Fig. 1. The schematic representation of the three-tiered bio-IPA supply chain. The supply chain comprises sugar beet supply counties, sugar processing plants, and IPA production facilities. The optimization objectives include the costs and emissions associated with various sources: biomass, transportation, sugar production, IPA synthesis, and CO_2 capture processes.

The supply chain is dissected into three interlinked components: resource assessment, logistic planning, and plant scale design. These components collectively address challenges posed by the uneven geographical distribution of feedstock and the need for emission and cost-efficient transportation. This study focuses on the development of a GIS-based supply chain optimization, tailored for biomass resources distribution, enhancing decision-making in plant scaling and logistic efficiencies.

2.1. Overview of the sugar beet-to-IPA supply chain model

2.1.1. Spatial information of the sugar beet to IPA supply chain system

The Red River Valley region is the most well-known sugar beet production area in the United States (Townsend, 1918). Minnesota is one of the states that produce the most sugar beets, providing 11,145, 000 mt in 2020, or 33.15 % of the nation's total production (Beef2Live. (n.d.) 2023). There are 25 counties in Minnesota cultivating sugar beets (United States Department of Agriculture 2023). The primary area for sugar beet production in Minnesota is the northwest region (Fig. 2a.) and the cost of sugar beet production is lower in this region (Fig. 2b.).

In terms of processing, five major sugar production factories process raw sugar beets into sugar suitable for the food industry (Fig. 3.). The idea of producing IPA via fermentation opens up new possibilities for sugar to various applications. The 19 existing ethanol fermentation plants (Minnesota Bio-Fuels Association, 2023) in the state have been suggested as potential locations for IPA plants (Fig. 3.). This choice is motivated by several strategic advantages. Firstly, the ethanol fermentation plants already have a significant portion of the required infrastructure for IPA production, including fermentation tanks, distillation systems, and other essential process equipment (De Jong et al., 2012). Repurposing these facilities offers a cost-saving avenue compared to initiating new constructions. Secondly, the raw materials for both ethanol and IPA production processes, primarily sugar beet or grains, are similar, ensuring that existing supply chain and logistics structures remain relevant (Liebeck et al., 2008). Thirdly, the workforce employed in ethanol fermentation plants possesses skills that align well with the demands of IPA production, making the transition smoother and obviating the need for extensive retraining or new hiring processes (Liebeck et al., 2008). Lastly, from a regulatory standpoint, these fermentation plants, having already secured environmental and safety approvals, are poised for a relatively seamless transition to IPA production (Liebeck et al., 2008).

In this study, the sugar beet-to-IPA supply chain is structured across three tiers (Fig. 3): from the sugar beet cultivation counties to the beet sugar production plants, and from sugar production plants to sugar-based IPA fermentation plants. The design is focused on identifying and implementing the most cost-effective and environmentally efficient configuration for the supply chain, ensuring optimal resource utilization.

2.1.2. Distance estimations in supply chain transportation

Efficient transportation is essential in optimizing the supply chain, and distance measurement plays a crucial role in achieving this. In the context of the sugar beet-to-IPA supply chain, it is important to have good estimates of the distances between different sites: from the sugar beet supply counties to sugar production plants and then to the potential IPA sites.

The study applies the direct linear distance, which refers to the shortest distance between two points on the Earth's surface. This is a simplification compared to the more accurate information provided by tools like the Google Maps Distance Matrix API (Allman et al., 2017; Google, 2017), which accounts for actual road routes. Although the direct linear distance may not reflect the actual road or transportation distances, which can be influenced by various geographic or infrastructural constraints, it provides an initial, unobstructed distance approximation. This approximation is particularly useful in the preliminary stages of supply chain planning, where the precise road or navigational details might be irrelevant and can be addressed in later,

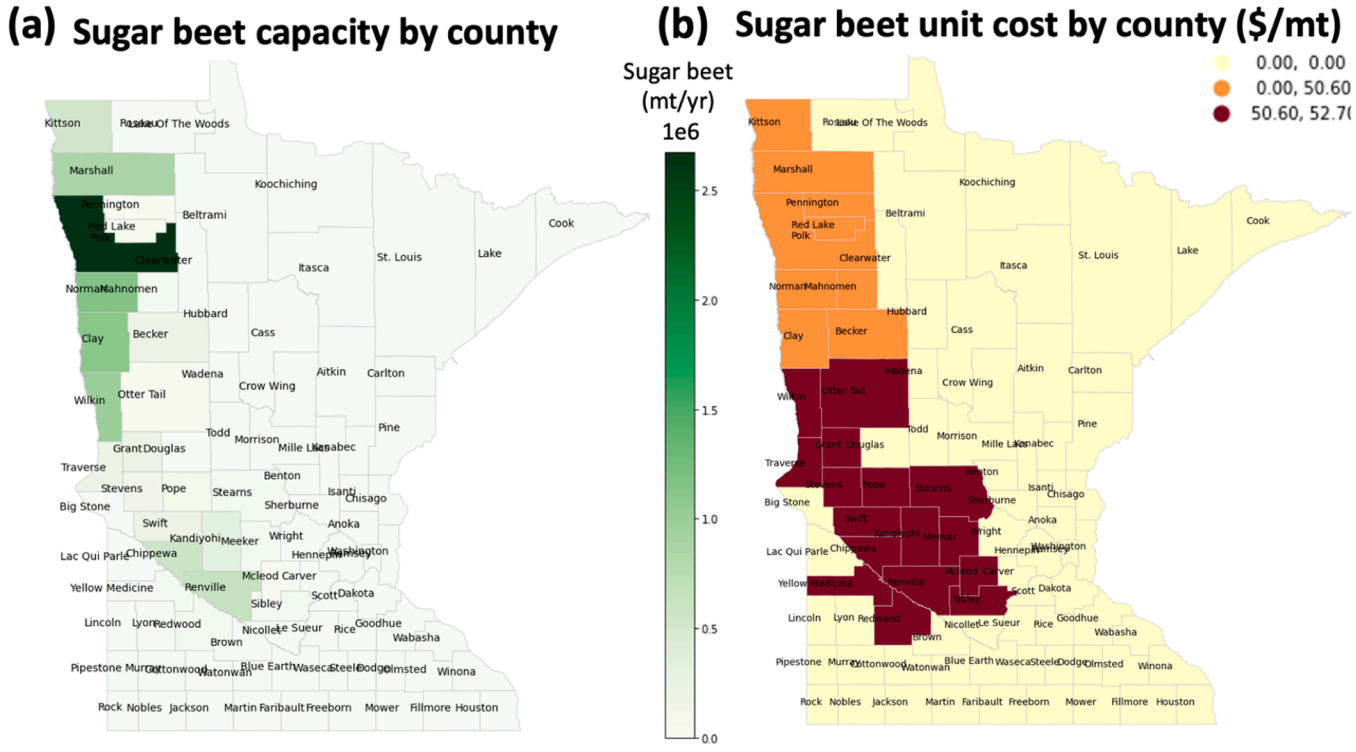

Fig. 2. Distribution of sugar beet availability and price across counties in Minnesota. Fig. 2a illustrates the sugar beet capacity by county, measured in metric tons, showcasing the geographical distribution and production potential within Minnesota. Fig. 2b displays the unit cost of sugar beet production by county, denoted in USD per metric ton, highlighting the cost variability across different regions. The color gradients in both maps reflect the respective scales of capacity and cost.

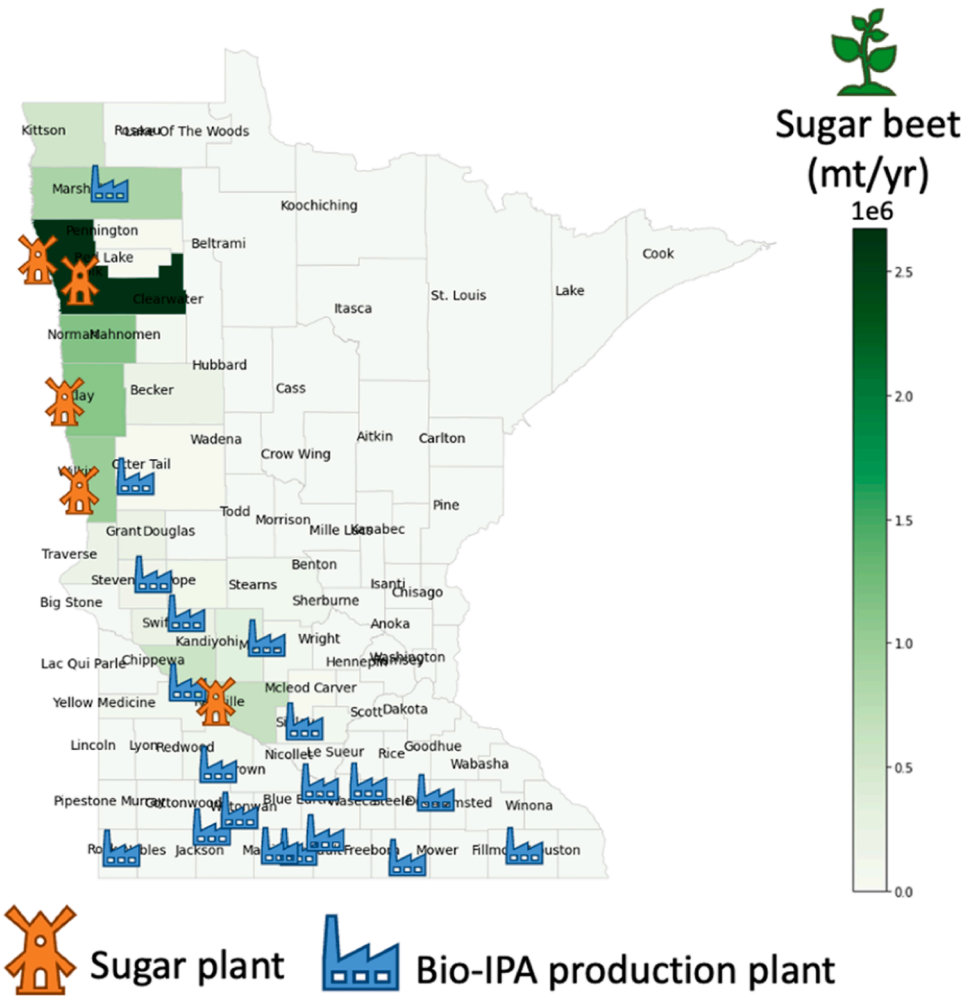

Fig. 3. The sugar beet-to -IPA supply chain configuration.

more detailed analyses.

To calculate the direct linear distance accurately across the Earth's curved surface, the study uses the haversine formula (Kahn et al., 1975). This mathematical function determines the great-circle distance between two geospatial points based on their longitudes and latitudes, accounting for the Earth's spherical nature (Kahn et al., 1975). The required geospatial data, specifically the latitudinal and longitudinal coordinates of sugar production sites and potential IPA plant locations, were obtained from OpenCage Geocoder (OPENCAGEGEO, 2016). This tool enables the conversion of location names into their respective geospatial coordinates and vice versa. To simplify the integration of sugar beet resource data with the transportation network data, the study assumes that all feedstock produced within a county is concentrated at the county's geographical center. Although this assumption provides a practical means of managing large datasets, it abstracts many complexities. For intra-county transportation distance approximations, the radius of a circle equivalent in area to the county serves as the representative distance.

2.2. System overview and cost estimation

Techno-economic analysis (TEA) evaluates the technical and economic feasibility of the bio-IPA production process. TEA merges engineering design insights with thorough financial assessments to determine the commercial viability of a technology. For bio-IPA production, the cost estimation involves conceptual process design, leading to a detailed process flow diagram. Equipment sizing and capital expenses are calculated using material and energy balances, applying a power-law scaling exponent of 0.7, informed by NREL 2021 design cases (Turchi et al., 2021). The financial analysis considers a 30-year plant life, a 21 % income tax rate, and a 5 % annual increase in working capital based on the fixed investment. (Supporting Information for more assumption of the TEA)

2.2.1. Synthetic Syntrophic consortium for efficient IPA production from sugars and the cost estimation

Building on the pioneering research by Charubin and Papoutsakis, (2019), this study focuses on the potential of the two-strain syntrophic consortium involving *C. acetobutylicum* (*Cac*) and C. *ljungdahlii* (*Clj*) for the production of bio-alcohols. *CaC* is notable for its ABE (acetone-butanol-ethanol) fermentation process, efficiently converting a variety of sugars, including sucrose and glucose, into acetone, butanol, and ethanol (Moon et al., 2016). The broad sugar utilization capability enhances the process's flexibility and efficiency, making *CaC* a versatile and robust microorganism for industrial bioprocessing applications. Moreover, one of the significant attributes of this consortium system was its proficiency in CO_2 fixation, ensuring optimal utilization of all carbon and electrons present in the sugar substrate. Within the co-culture, *Clj* effectively transformed all the acetone produced by *Cac* into isopropanol (IPA). Further, *Clj* enabled undergoes the Wood-Ljungdah pathway to metabolize CO_2 and H_2, leading to the production of acetate and a minor fraction of ethanol (Charubin and Papoutsakis, 2019).

Expanding on this, the technology (Minnesota Bio-Fuels Association, 2021) draws inspiration from the synthetic syntrophic consortia of

Clostridium organisms. The ultimate objective is the comprehensive utilization of the carbon and electrons within the substrate, along with the consumption of an additional 3 mol CO_2 for every mol 6C-sugar by harnessing electrons from H_2. Stable microbial consortia predominantly based on *Clostridium* organisms are poised to achieve this and potentially fix an even higher amount of CO_2 per mol sugar. Based on data references (Lee et al., 2012), the monoculture demonstrates that for every mole of glucose consumed, a mole of IPA and three moles of CO_2 are produced. To achieve the carbon neutral, the syntrophic *Cac/Clj* coculture, with its ability to fix 3 mol CO_2 per mol glucose ($+H_2$), manifests a total product formation rate of 31 mM/h, governed by the stoichiometric equation:

$$1\text{Glucose} + 3CO_2 + 13.99H_2 \rightarrow 2.28\text{IPA} + 0.57\text{EtOH} + 0.50\text{Acetate} + 8.14\text{H2O}$$

Relying on the stoichiometric equation and adopting a feed rate of 18,000 mt sugar/yr as a benchmark case (with a glucose to IPA ratio of 73 wt.%), a production yield of 16,350 mt IPA-ethanol/yr was anticipated. To contextualize, aiming to replace 25 % of the US's IPA production with biomass-based production would necessitate approximately 186,000 mt/yr of sugar, grounded on the net stoichiometric equation. To simulate the production process of the synthetic syntrophic consortia, a model was created using Aspen Plus® V12 simulation software (Fig. 4). The simulation considers raw material and energy metrics for techno-economic analysis (TEA). The IPA production process includes a bioreactor, a beer column (D-1) to separate 99 wt.% of water and acids (acetate, which is typically present in the broth as acetic acid) from fermentation flows, and distillation towers (D-2 and d-3) for purification. As two binary azeotrope systems are formed (IPA/H_2O and EtOH/H_2O), ethylene glycol was identified as an excellent extractant in the extracted distillation design (Ma et al., 2019), breaking the azeotropes and increasing the relative volatility of the alcohol-water mixture.

2.2.2. The cost estimation of CO_2 sourcing from ethanol plant

In Minnesota, the total CO_2 emission from the ethanol fermentation process stands at 3.65 million mt/yr (McPherson, 2010). The CO_2 stream derived from fermenting corn and biomass to yield ethanol has a purity of 99.9 % and requires minimal processing before it is ready for compression and pipeline transport. Moreover, it is assumed that CO_2 was obtained directly from the ethanol plant and that there are no transportation costs associated with it. However, based on this supposition, the CO_2 emissions from the ethanol facilities limit the IPA plant's production capacity. The cost and capital expenditure associated with CO_2 capture are proportional to the plant's scale. The relationship is mathematically captured through the equation: Capital Expenditure ($Million) = 0.15 × Plant Size (Million Gallons per Year) + 9. In this research framework, the operational costs, which comprise capture, compression, and dehydration derived from ethanol plants, are estimated to be $8.58 per metric ton of CO_2 processed (McPherson, 2010).

2.2.3. Beet sugar production process and cost estimation

Though beet sugar is primarily composed of sucrose, *Cac* can metabolize sucrose through its metabolic pathways (Wang and Yin, 2021). Sucrose, being a disaccharide of glucose and fructose (both 6-C sugars), can be broken down by these bacteria into monosaccharides, which then enter central metabolic pathways like glycolysis (Wang and Yin, 2021; Kádár and Fonseca, 2019). Using sucrose may reduce the complexity of the feedstock preparation process compared to using more complex carbohydrates. This simplification can lead to lower processing costs and easier scalability.

Sugar production begins with extracting sugar from sliced beets using hot water, resulting in raw juice (Cheng et al., 2019). This juice is purified by adding calcium hydroxide and carbon dioxide, which removes impurities. The purified juice is then concentrated through evaporation under vacuum conditions. In the crystallization stage, sugar crystallizes out in a vacuum, forming a mixture of crystals and syrup (Eggleston and Lima, 2015). Centrifugation separates these components, and the sugar crystals are washed and dried with hot air. The final product is cooled to produce granulated sugar (Eggleston and Lima, 2015). Drawing insights from Shield, (2016), the economics of sugar production are mapped from crop cultivation to refining stages. Shield's study distinguishes between fixed capital and variable costs, highlighting the economies of scale that favor larger processing plants with reduced unit costs. Applying a power relationship of 0.7, as proposed by Shield, allows for estimations of these costs across varied scales of sugar production, essential for informed decision-making in bio-IPA production. The impact of economies of scale is captured by the power relationship, where larger processing plants benefit from reduced unit costs. A power relationship of 0.7 is used to represent this scalability function (Supporting Information).

2.2.4. Transportation cost estimation

An efficient transportation system is a vital component of a well-functioning supply chain that ensures goods are delivered promptly and cost-effectively. With several modes of transport available, each mode has its unique cost implications that impact the overall transportation cost. In this study, we have chosen trucks as the preferred mode of transport within the supply chain. The cost of transportation varies based on several factors, including distance, shipment dimensions, and weight (Ghafoori et al., 2007). In general, it costs more to transport larger or heavier shipments over longer distances (Ghafoori et al., 2007). To determine the distance between sites, geospatial information comes in handy, and it is a useful tool in calculating transportation costs.

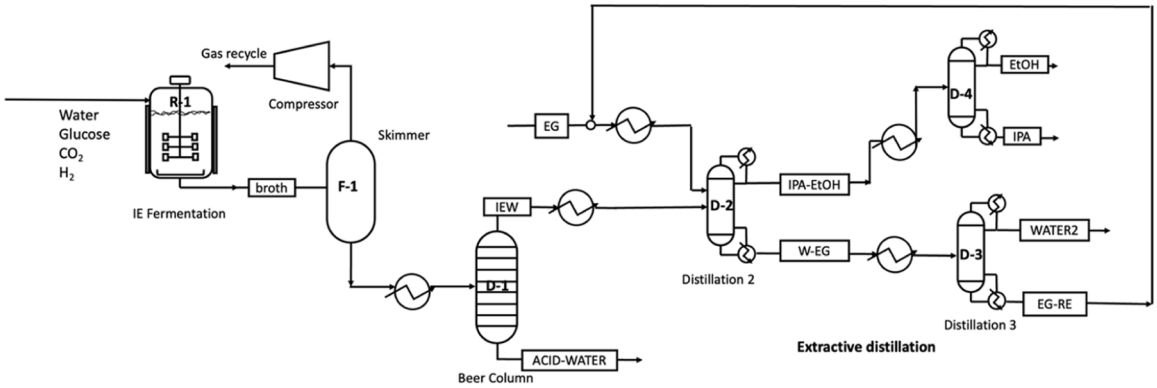

Fig. 4. Process flowsheet and flow results of IPA/EtOH production with 3 mol CO_2 fixed per mol glucose. The plant's capacity is 18,000 mt/year of glucose and operates in a continuous mode for 8000 h per year. We assume a plant's economic life is 30 years.

The transportation cost structure consists of two critical components: fixed costs and variable costs. Fixed costs remain constant, tied to truck loading and unloading, and do not change with the distance traveled. Variable costs, on the other hand, change in line with the distance covered and can be expressed in dollars per tons-kilometer or dollars per ton for each hour of operation assuming a consistent average transit speed. These components are known as the distance fixed cost and distance variable cost. It's worth noting that the size of the truck does not affect the scale of distance fixed cost and distance variable cost for trucking.

When it comes to transporting sugar beets, the variable transportation cost is $0.25 per mt-km, while the fixed cost is $3.19 per mt, inclusive of loading and unloading charges (Ghafoori et al., 2007). On the other hand, for sugar, the variable transportation cost is $0.09 per mt per km, with the fixed cost at $6.6 per mt (Ghafoori et al., 2007). The disparity in transportation costs between sugar beets and sugar is a result of several underlying factors. Processed sugar is denser than sugar beets, leading to more complex and sturdy packaging to prevent moisture absorption and contamination, which inevitably increases the costs. Furthermore, sugar is more sensitive to environmental variables and requires specialized handling protocols during transportation, necessitating higher fixed costs.

2.3. Life cycle assessment (LCA)

This section summarizes the Life Cycle Assessment (LCA) of sugar-based IPA technologies in the U.S. market. To measure the environmental impact of these processes, we utilized the open-source framework, Brightway2 (Mutel, 2017). The Ecoinvent® v3.9.1 (Wernet et al., 2016), life cycle inventory database was used to measure the environmental footprint of the process. We considered the growth of biomass, raw material pretreatment, upstream utility generation, transportation emissions of the raw materials, and the bio-IPA production phase, with the system boundary extending from cradle-to-gate.

The focused environmental impact category is GHG emissions. We assessed the impacts of climate change by ReCiPe midpoint method (Borghesi et al., 2022) as the global warming potential is the most concerned environmental issue and more relevant to policies and legislation (Cherubini et al., 2012). The life cycle inventory for the U.S. glucose market includes the CO_2 sequestration of sugar beet during growth, and emissions from harvesting, refining, and transportation. Based on the Ecoinvent database, sugar beet production results in 0.079 kg of CO_2-eq per kg of sugar beet, and beet sugar production, excluding feedstock emissions, produces 0.19 kg of CO_2-eq per kg of sugar. More information and assumptions on LCA can be found in the supporting documentation.

2.4. Optimization model formulation

In this work, the model was developed on GAMS platform (Boisvert et al., 1985) and solved with the CPLEX solver (Anand et al., 2017). The optimization of the sugar beet-to-isopropanol supply chain problem is formulated as a multi-objective MILP problem ((ii) case) that is subject to constraints corresponding to the mass balances, the capacity range of the facilities, techno-economic evaluation, environmental impact assessment, and network configuration constraints. The economic objective function is to minimize the unit production cost, which involves the raw material cost, transportation cost, and IPA production cost. The environmental objective function is to minimize unit GHG emissions evaluated by the ReCiPe method with the global warming potential indicator (GWP100) (Allen et al., 2016). All sets, subsets, parameters, and variables used in the sugar beet-to-isopropanol supply chain problem are given in the Nomenclature section. The detailed mathematical model formulation is shown in Eqs. (3)-(37). The objective of the optimization model is to minimize annual biomass-based IPA production costs ($obj_{economic}$) and the GHG emissions of the production of IPA (obj_{gwp})

$$min\ obj_{economic} = \frac{total\ production\ cost}{total\ production\ capacity} \tag{1}$$

$$min\ obj_{gwp} = \frac{net\ production\ emissions}{total\ production\ capacity} \tag{2}$$

s. t. Mass balance constraints
Capacity range of the facilities constraints
Techno-economic performance evaluation constraints
Life cycle assessment performance evaluation constraints
Network configuration constraints

2.4.1. Mass balance constraints

To illustrate the balance of mass within the three-level supply chain structure, different mass flows, such as "FS" and "SI" flows, are used to represent the relationship between sugar beet farms at the county level (F) to sugar plants (S) and sugar plants to IPA production sites (A). Set I denotes the sugar beet supply county options; set J represents the sugar production sites, and set K denotes the potential IPA biorefinery plants built neighbor the existing ethanol plants. While set L indicates the facility capacity levels, segment the capacity levels of the sugar beet production sites and IPA biorefinery into small, medium, and large levels. Within each level, there is an estimated fixed capital cost and a variable capital cost that will be linearly proportional to the capacity (Lin et al., 2013). The target capacity of IPA is variable. Therefore, a continuous variable, s, is introduced to serve as the scaling factor for determining how many 141,360 mt of the IPA is produced (For detailed information on the conversion from sugar to isopropanol (IPA) product flow, please refer to the Supporting Information.). The total possible consumption amount of sugar beet by counties that transport to sugar plants ($flow^{FS}_{i,j}$) is limited by the availability of sugar beet in each county (b_i) (Eq. (3)). Additionally, to meet the production target, the total quantity of sugar beet should be equal to the required biomass supply (BS) (Eq. (4)). The required processing sugar beet ($\sum_i flow^{FS}_{i,j}$) or sugar ($\sum_j flow^{SA}_{j,k}$) amount should also equal the sum of the capacity of the facilities of sugar plants ($s^S_{j,l}$) and IPA biorefinery ($s^A_{k,l}$) at all levels (Eqs. (5) and (6)). Eqs. (7) and (8) demonstrate that the sum of the capacities of the sugar plants and biorefineries at all levels is equal to the total required amount of sugar beet (BS) and sugar (SS) for producing IPA, respectively. In this study, it is assumed that the raw materials cannot be shared between the same tier level of the supply chain, meaning that transported sugar beet cannot be transported to another sugar plant. Thus, the site-to-site mass balance can be expressed as in Eq. (9), where α (Sucrose makes up roughly 14 to 20 % of a root's weight; an assumed value of 20 % is used in this study (Campbell, 2002)) represents the weight loss conversion of sugar beet to sugar. Therefore, according to the stoichiometry outlined in Section 2.2.1, SS is 244,000 mt of sugar for producing 141,360 mt of IPA, with SS constitutes 20 wt.% of BS.

$$\sum_j flow^{FS}_{i,j} \le b_i,\ \forall i \in I;\ \forall j \in J \tag{3}$$

$$\sum_i \sum_j flow^{FS}_{i,j} = BS \times s,\ \forall i \in I;\ \forall j \in J \tag{4}$$

$$\sum_i flow^{FS}_{i,j} = \sum_l s^S_{j,l},\ \forall i \in I;\ \forall j \in J;\ \forall l \in L \tag{5}$$

$$\sum_j flow^{SA}_{j,k} = \sum_l s^A_{k,l},\ \forall j \in J;\ \forall k \in K;\ \forall l \in L \tag{6}$$

$$\sum_j \sum_l s^S_{j,l} = BS \times s,\ \forall j \in J;\ \forall l \in L \tag{7}$$

$$\sum_k \sum_l s^A_{k,l} = SS \times s,\ \forall k \in K;\ \forall l \in L \tag{8}$$

$$\sum_i flow^{FS}_{i,j} \times \alpha = \sum_k flow^{SA}_{j,k},\ \forall i \in I;\ \forall j \in J;\ \forall k \in K \tag{9}$$

2.4.2. Capacity range of the facility constraints

Eqs. (10)-(15) describe the capacity range of facilities at different levels: small, medium, and large (indexed by l in set L). The user-defined values, ζ, vary depending on the case represents the maximum and minimum capacity of a facility level. For example, for sugar plant facilities at a small capacity level, the capacity ($s^S_{j,l=small}$) falls within the range of $\zeta^{S,min}_{l=small}$ and $\zeta^{S,max}_{l=small}$, where $\zeta^{S,min}_{l=small}$ and $\zeta^{S,max}_{l=small}$ represent the minimum and maximum capacity limits of the range, respectively (the parameter values defined by the user are detailed in the Supporting Information). Binary variables $e^S_{j,l}$ and $e^A_{k,l}$ are employed to activate these capacity constraints only when a facility is selected, enhancing the model's decision-making flexibility.

Furthermore, the model also adapts to real-world conditions by factoring in domestic sugar demand, ensuring the sugar allocation for facilities is realistic (e.g., $\zeta^{S,min}_l$ and $\zeta^{S,max}_l$ are adjusted by a coefficient reflecting the portion of production capacity not allocated for domestic sugar market use.). This adjustment accounts for the operational flexibility in responding to market demand variations. It maintains a focus on the practical application of converting sugar surplus into biotechnological commodities, without assuming any growth beyond what current supply data indicates. By calibrating sugar quantities to the actual needs of the domestic market, the model avoids underestimating production capacities, which could result if it only considered sugar reserved for bioprocessing. This application is optional, details on how the factor is determined are elaborated in the Supporting Information. Additionally, it is crucial to acknowledge the potential market disruption resulting from reallocating the sugar supply originally designated for export to isopropanol production. Although a comprehensive analysis of the impact on global food supply and market dynamics is beyond the scope of this study, the significance of this potential disruption cannot be overlooked.

Eqs. (10) describe the capacity ranges of sugar plant facilities, while Eqs. (11) describe the capacity level constraints of the IPA biorefinery.

$$\zeta^{S,min}_l \times e^S_{j,l} \le s^S_{j,l} \le \zeta^{S,max}_l \times e^S_{j,l},\ \forall j \in J; \forall l \in L \tag{10}$$

$$\zeta^{A,min}_l \times e^A_{k,l} \le s^A_{k,l} \le \zeta^{A,max}_l \times e^A_{k,l},\ \forall k \in K;\ \forall l \in L \tag{11}$$

2.4.3. Techno-economic performance evaluation constraints

The economic objective of the sugar beet-to-isopropanol supply chain is to minimize the unit production cost (Eq. (1)), which is comprised of five costs: sugar beet purchase costs (C^F), transportation-related costs (C^T), sugar production costs (C^S), CO_2 capture related costs (C^G), and biorefinery-related costs (C^A). Therefore, the total production cost is described as Eq. (12).

$$\textit{total production cost} = C^F + C^T + C^S + C^G + C^A \tag{12}$$

The sugar beet purchase costs (C^F) are formulated as Eq. (13) with variables of the optimal flow configuration ($flow^{FS}_{i,j}$, the amount of sugar beet by counties i that transport to sugar plant j) from the sugar beet farms to sugar plant sites and the sugar beet cost at sourcing county (c_i).

$$C^F = \sum_i \sum_j flow^{FS}_{i,j} \times c_i,\ \forall i \in I;\ \forall j \in J \tag{13}$$

The transportation costs (C^T) involve fixed transportation costs (C^{Tf}), and variable transportation costs (C^{Tv}) that is a function of the amount of goods transported, and the distance covered, as described in Eq. (14). The fixed costs, C^{Tf}, remain constant regardless of the quantity or distance of goods transported, reflecting expenses that do not fluctuate with the transportation activity, such as administrative fees or the cost of maintaining vehicles (Gray, 1971). In contrast, the variable costs, C^{Tv}, are directly influenced by the volume of goods transported and the distance covered, encompassing expenses like fuel and labor, which vary with the scale of transportation operations (Gray, 1971). The distances between the sites d_{ij} (distance between a sugar beet supply county and a sugar plant) and d_{jk} (distance between a sugar plant and a bio-IPA plant) are determined using their respective latitudinal and longitudinal coordinates. Specifically, the haversine formula is employed to describe the great-circle distance between two points on a sphere based on their longitudes and latitudes. Both variable and fixed transportation costs are user-defined. Eq. (15) describes the fixed transportation costs with unit cost $C^{FS,Tf}$ and $C^{SA,Tf}$ (in $/mt), varying with the types of transporting goods: sugar beet and sugar; respectively. Eq. (16) describes the variable transportation costs ($C^{FS,Tv}$ and $C^{SA,Tv}$ in unit of $/ mt-km), as a function of the transportation distance, and the amount of goods being transported ($flow^{FS}_{i,j}$ and $flow^{SA}_{j,k}$) (Eq. (16)).

$$C^T = C^{Tf} + C^{Tv} \tag{14}$$

$$C^{Tf} = \sum_i \sum_j flow^{FS}_{i,j} \times C^{FS,Tf} + \sum_j \sum_k flow^{SA}_{j,k} \times C^{SA,Tf},\ \forall i \in I;\ \forall j \in J;\ \forall k \in K \tag{15}$$

$$C^{Tv} = \sum_i \sum_j flow^{FS}_{i,j} \times C^{FS,Tv} \times d_{ij} + \sum_j \sum_k flow^{SA}_{j,k} \times C^{SA,Tv} \times d_{jk},\ \forall i \in I;\ \forall j \in J;\ \forall k \in K \tag{16}$$

The sugar production costs (C^S) include the operating cost (C^{So}) and the capital costs (C^{Sc}) (Eq. (17)). In this study, capital costs, particularly in the context of manufacturing, processing, or infrastructure development, can be segmented into fixed and variable components, where the variable capital costs ($C^{Sc,v}_l$) can be approximated as being linear over three capacity level ranges. The linear dependence assumption simplifies the modeling and forecasting processes while segregating capital costs into fixed and variable components provides a more comprehensive understanding of the investment required at different operational scales. Thus, the capital cost is represented as the sum of fixed and variable costs and a factor θ, estimating annual capital charges for assets that have multi-year lifetimes (Eq. (18)). θ serves as an annualization factor, distributing capital costs across an investment's useful lifetime. In this study, θ is set at 13.5 %, calculated using the discounted cash flow (DCF) method. This value considers variables such as inflation, interest rates, and opportunity costs, using a discount rate of 12 % over a 30-year span. On the other hand, the unit operating cost ($C^{So,unit}$) is assumed to be the same under different levels of capacity design. Therefore, the total operating cost is proportional to the annual sugar beet demand (Eq. (19)). Similarly, the IPA biorefinery production cost (C^A) can be formulated as the operating cost (C^{Ao}) and the capital costs (C^{Ic}) (Eq. (20)). The capital cost comprises with the fixed ($C^{Ac,v}_l$) and variable costs ($C^{Ac,f}_l$) (Eq. (21)). The annual operating costs of the IPA biorefinery are linear with the total required sugar amount, (SS), as Eq. (22) formulated.

$$C^S = C^{So} + C^{Sc} \tag{17}$$

$$C^{Sc} = \theta \times \left(\sum_j \sum_l C^{Sc,v}_l \times s^S_{j,l} + C^{Sc,f}_l \times e^S_{j,l} \right),\ \forall j \in J;\ \forall l \in L \tag{18}$$

$$C^{So} = C^{So,unit} \times BS \times s \tag{19}$$

$$C^A = C^{Ao} + C^{Ac} \tag{20}$$

$$C^{Ac} = \theta \times \left(\sum_k \sum_l C_l^{Ac,v} \times s_{k,l}^A + C_l^{Ac,f} \times e_{k,l}^A \right), \ \forall k \in K; \ \forall l \in L \tag{21}$$

$$C^{Ao} = C^{Ao,unit} \times SS \times s \tag{22}$$

Except for the beet sugar as the main raw material for producing IPA in the co-culture system, CO_2, fixed by the *Clj*, serves as an additional carbon source and enhances the overall efficiency and sustainability of the production process. The CO_2 is sourced from ethanol plants, that are neighboring to the selected IPA plants. The cost of capturing the CO_2 is formulated as a summation of a fixed cost ($C_l^{G,v}$) and variable cost ($C_l^{G,f}$) that is linearly dependent on the demand of the sugar ($s_{k,l}^A$). The CO_2 capture cost (C^G) is described as shown in Eq. (23), where β is the weight ratio of CO_2 to sugar in the stoichiometric equation.

$$C^G = \sum_k \sum_l \beta \times C_l^{G,v} \times s_{k,l}^A + C_l^{G,f} \times e_{k,l}^A \tag{23}$$

2.4.4. Life cycle assessment performance evaluation constraints

In the sugar beet-to-IPA supply chain, the system boundary is from cradle-to-gate, meaning that the analysis encompasses all stages from the cultivation and harvesting of sugar beets, their transportation and processing, right through to the production of isopropanol (IPA), including all intermediate processes and inputs. This approach ensures a comprehensive assessment of the environmental impacts and resource use associated with the entire production lifecycle, up until the point where the IPA is ready for distribution or sale.

The environmental objective of the sugar beet-to-isopropanol supply chain is to decrease GHG emissions per unit, as outlined in Eq. (24). There are five sources of emissions, which are sugar beet (G^F), transportation-related (G^T), sugar production (G^S), CO_2 capture-related (G^G), and biorefinery-related (G^A). Therefore, Eq. (24) defines the total production emissions. $\lambda^{sugar\ beet}$ represents the environmental impact of producing sugar beet, and Eq. (25). describes the total emissions from sugar beet production. Two primary transportation routes contribute to transportation emissions: one from the county of the sugar beet farms to the sugar plant (d_{ij}) and the other from the sugar plant to the IPA biorefinery (d_{jk}). The cumulative transportation emissions are multiplied by the factor λ^{truck}, which is expressed in units of CO_2-eq/mt-km, as shown in Eq. (26). The sugar production emissions, excluding raw material emissions, are defined in Eq. (27). λ^{sugar} represents the unit emissions of beet sugar production, sourced from the EcoInvent database. This database provides allocation results from a plethora of industrial emission data and literature. In this study, the emissions from the IPA biorefinery technology have not yet been implemented in real-world scenarios. Therefore, a power law scale factor is used to represent the emissions, which represents the effects of design size on emissions (Caduff et al., 2014; Bahlawan et al., 2021). Additionally, a piecewise linearization method is employed to present the emission of the IPA production (λ_l^{IPA}) more effectively (Eq. (28)). Conversely, the utilization of carbon dioxide will yield a net negative emission, denoted as G^G. The term $\lambda^{carbon\ capture}$ represents the carbon emissions originating from carbon capture process. Eq. (29) represents the contributions relating to CO_2 capture-related GHG emissions. Furthermore, the availability of carbon dioxide amount is limited by the emissions of the ethanol sites, represented as $D_k^{CO_2}$ (Eq. (30)).

$$net\ production\ emissions = G^F + G^T + G^S + G^G + G^A \tag{24}$$

$$G^F = \sum_j flow_{i,j}^{FS} \times \lambda^{sugar\ beet} \tag{25}$$

$$G^T = \sum_i \sum_j flow_{i,j}^{FS} \times \lambda^{truck} \times d_{ij} + \sum_j \sum_k flow_{j,k}^{SA} \times \lambda^{truck} \times d_{jk}, \ \forall i \in I; \ \forall j \in J; \ \forall k \in K \tag{26}$$

$$G^S = \sum_j \sum_l s_{j,l}^S \times \lambda^{sugar}, \ \forall j \in J; \ \forall l \in L \tag{27}$$

$$G^A = \sum_k \sum_l s_{k,l}^A \times \lambda_l^{IPA}, \ \forall k \in K; \ \forall l \in L \tag{28}$$

$$G^G = \sum_j \sum_k \beta \times flow_{j,k}^{SA} \times \lambda^{carbon\ capture}, \ \forall j \in J; \ \forall k \in K \tag{29}$$

$$\sum_j \beta \times flow_{j,k}^{SA} \le D_k^{CO_2}, \ \forall j \in J; \ \forall k \in K \tag{30}$$

2.4.5. Network configuration constraints

Network configuration constraints refer to a set of rules or conditions that dictate the formation and operation of a network, particularly in mathematical modeling, optimization problems, and system design. In the context of optimization, constraints can help in determining the optimal configuration of a network under certain conditions. In network design problems, binary variables represent decisions for path selection and operational decisions. e_i^F stands as a binary variable indicating the presence of a chosen sugar beet supply county. Eq. (31) guarantees the selection of sugar beet farms (e_i^F) that establish connects with their corresponding sugar plants. *bigM* is a large constant used to enforce non-strict inequalities, while *eps* represents a small positive number to ensure strict inequalities in the optimization model. Further, e_j^S and e_k^I serve as binary variables representing the selection of the sugar plant and biorefinery site, respectively. The sum of the operational sites at all levels is equal to the number of all sites at the supply chain configuration (Eqs. (32) and (33)). These representations illustrate the intricate interplay of variables and constraints that determine the optimal structure and operations of a network, ensuring efficiency and alignment with objectives.

$$e_i^F \times eps \le \sum_j flow_{i,j}^{FS} \le e_i^F \times bigM + eps, \ \forall i \in I; \ \forall j \in J \tag{31}$$

$$\sum_l e_{j,l}^S = e_j^S, \ \forall j \in J; \ \forall l \in L \tag{32}$$

$$\sum_l e_{k,l}^A = e_k^A, \ \forall k \in K; \ \forall l \in L \tag{33}$$

3. Results

This study conducts a preliminary TEA and LCA for the proposed innovative bio-IPA production technology. These analyses provide a reasonable estimation of the production costs, operating costs, and GHGs intensity of bio-IPA production at various levels. The preliminary TEA for the bio-based IPA process indicates that raw materials, such as glucose priced at $0.33/kg (Cheng et al., 2019), account for 41 % of the bioprocess cost. Additionally, ethanol by-product sales at $960/mt (Global chemical industry) significantly offset operating costs, and the cost of CO_2 is considered free due to tradeable federal tax credits. It should be noted that the cost and emissions of hydrogen were assumed to be free and zero-emission in this study. This assumption is based on the hydrogen required for the process being sourced from a combination of renewable sources and fermentation off-gas. Specifically, a portion of the hydrogen is derived from the fermentation off-gas generated by *Clostridium acetobutylicum* (Minnesota Bio-Fuels Association, 2021), which helps meet some of the CO_2 fixation hydrogen demands. The additional hydrogen needed is assumed to be obtained from renewable

sources, such as water electrolysis powered by renewable energy, aligning with the US Department of Energy's hydrogen hubs projects (Lewis, 2024)and the ARPA-E program (Minnesota Bio-Fuels Association, 2021). These initiatives aim to accelerate the commercial-scale deployment of low-cost, clean hydrogen and establish networks of clean hydrogen producers, consumers, and infrastructure. In comparison, the preliminary TEA shows that the traditional industrial process using propene via indirect hydration pathway (Kropf, 1966), priced at $0.584/kg, incurs higher raw material costs for producing IPA. The comprehensive cost breakdown (more details in Supporting Information) reveals that the bio-based process benefits from lower raw material and utility costs (accounting for 5 % of the total costs for bio-IPA production compared to 32 % for fossil-based IPA production), as well as efficient utilization of resources such as CO_2 and clean hydrogen. The preliminary TEA provides an economic comparison of bio-IPA and fossil-based IPA, establishing the parameters used for the subsequent analysis of the bio-IPA supply chain.

3.1. Techno-Economic and environmental optimization of bio-based IPA production

This section explores the TEA and LCA results and the constraints imposed by the production capacity of bio-IPA within the supply chain. By solving case (i), the MILP optimizes the parameter s, the scaling factor that determines the production of IPA in multiples of 141,360 mt of the IPA is produced, the analysis reveals that design capacities below 36,809.4 mt or exceeding 965,898 mt are infeasible due to operational scale limits at IPA and sugar processing plants. Within the feasible IPA capacity, the Pareto solution sets for varying IPA demand scenarios was performed with the use of ϵ-constraint method (case (iii)) as follows Yue et al., (2014).

$$\begin{aligned} &obj_{gwp} \le \epsilon \ (\text{kg } CO_2/\text{kg IPA}) \\ &\epsilon^L \le \epsilon \le \epsilon^U (\text{kg } CO_2/\text{kg IPA}) \end{aligned} \tag{34}$$

In the study, the ϵ-constraint method was employed for MILP due to

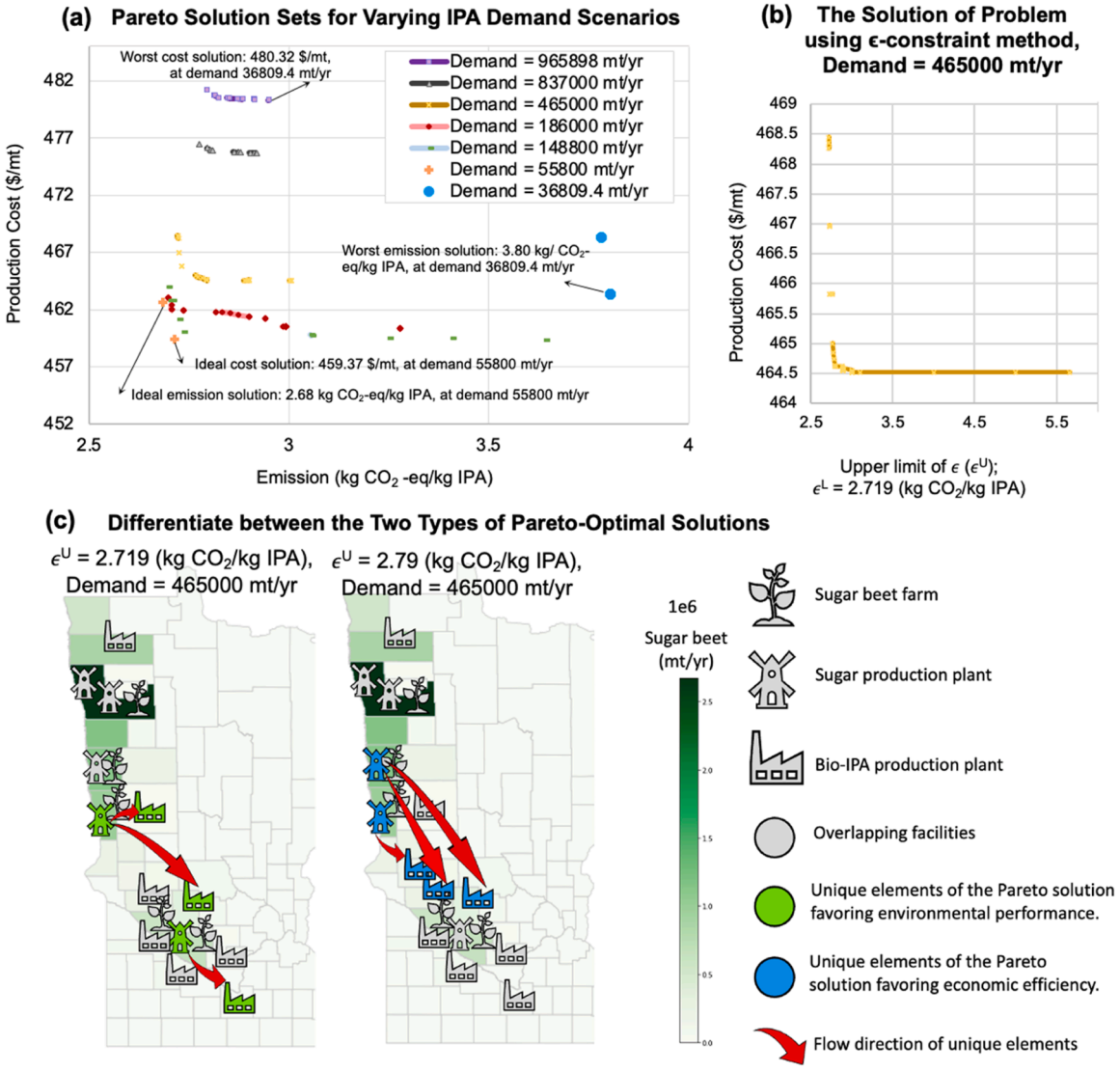

Fig. 5. Pareto Solution Sets for Varying IPA Demand Scenarios: Fig. 5a illustrates the trade-offs between cost and emissions for different annual IPA production demands. Each point and line represent Pareto optimal sets, where cost and emission objectives are balanced according to the ϵ-constraint method. The sets span across a range of IPA demands, from 36,809.4 mt/yr to 965,898 mt/yr, highlighting how the optimal trade-offs shift as the production scale increases. The ideal and worst solutions refer to the most and least favorable solutions within the set of all possible optimal solutions among the demand scenarios, respectively. (Fig. 5b): The optimal performance in IPA production costs, constrained by variable emission performance levels (ϵ^U); (Fig. 5c): The comparison of supply chain configurations between the Pareto solution sets. the green and blue color-coding is used to differentiate between the two types of Pareto-optimal solutions, with green for better environmental performance and blue for better economic performance. The grey color indicates where the configurations share common elements, allowing for a direct visual comparison of the differences in supply chain structure influenced by prioritizing different objectives.

the potential for Pareto optimal points to occur within the interior of the convex hull defined by integer feasible points (Lopes et al., 2020). The methodology involves reformulating Eq. (2). to integrate the lower and upper bounds of the ε parameter, which are derived by independently minimizing and maximizing the secondary objective function, obj_{gwp} (case (ii)). In the optimization model, the vector of ϵ values is constrained to range within the defined limits, specifically between the vector of lower bounds of emissions (in kg CO_2) per kg of IPA produced, ϵ^L, and the vector of upper bounds, ϵ^U. The ϵ-constraint method ensures the identification of weakly optimal solutions, moreover, it assures Pareto optimality when each objective function is equal to the corresponding ϵ parameter (Pappas et al., 2021).

As demonstrated in Fig. 5a, the economic viability peaks at a production scale of approximately 55,800 mt, corresponding to a cost of $459.37 per mt. Across varying scales, optimal production costs at the feasible IPA demand scenarios range from $459.37 to $480.32 per mt (Fig. 5a), with the highest cost being 4 % above the lowest. In terms of environmental impact, CO_2 emissions in optimized scenarios vary between 2.68 and 3.80 kg CO_2-eq/kg IPA (Fig. 5a). The most efficient emission performance occurs at 55,800 mt/year, whereas the least efficient is at 36,809 mt/year (Fig. 5a), indicating a 41 % emission increase in the least favorable scenario as captured by the Pareto optimal sets. It should be noted that the inclusion of integer variables in the multi-objective optimization framework may introduce discontinuities and non-convexities in the Pareto frontier. The analysis of Pareto solution sets typically reveals that advancements in production cost do not correspond equally with enhancements in CO_2 emission reductions during the balancing of economic and environmental objectives. For instance, at an IPA demand level of 186,000 mt/yr, an increasing of 0.58 kg CO_2-eq/kg IPA corresponds to a production cost reduction of $2.66/mt. In contrast, the optimal equilibrium, as depicted in Fig. 5a for an IPA demand of 465,000 mt/yr (referenced in Fig. 5b), suggests that an incremental emission increase of 0.071 kg CO_2-eq/kg IPA can result in a cost reduction of $3.82/mt. To further clarify the underlying factors contributing to these differentials, Fig. 5c displays the two optimized supply chain configurations for IPA production, resulting from a multi-objective Pareto analysis when ϵ^U is 2.719 and 2.790 respectively. The $\epsilon^U = 2.719$ configuration showcases where the supply chain has been optimized for lower emissions, while the $\epsilon^U = 2.790$ configuration illustrates optimization for cost-effectiveness in the Pareto solution set. The elements marked in green show the changes made to create a supply chain that's better for the environment, like having fewer bio-IPA production plants (e.g., a larger capacity level of bio-IPA production facilities) to reduce overall emissions. Conversely, the blue markers signify an economically driven optimization, where the supply chain is restructured to capitalize on cost-effective sugar sources. This is evident from the efficiently managing where sugar comes from. For example, because sugar beets are less expensive in the northwest part of Minnesota, despite a solitary sugar processing plant in that region, it makes sense to send sugar beets from this area to different sugar plants and then finally distribute sugar to bio-IPA plants to save the production cost. The Pareto solution sets allow for a comparative analysis of how each optimization criterion—environmental impact and cost-efficiency—alters the supply chain layout, providing insights into the trade-offs between these two objectives.

Regarding the IPA production amounts, the study of varying supply chain configuration designs under fluctuating capacity levels reveals uncertainty in their operational cost and environmental impacts. When compared with the U.S. IPA market prices, where the Free on Board (FOB) Texas price for IPA ranged between $1560–1570 per metric ton in September 2023 (ChemAnalyst 2023), the economic advantage of bio-based IPA production becomes evident. Additionally, when considering the greenhouse gas emissions from traditional IPA synthesis methods, which for direct and indirect hydrogenation processes amount to 3.27 kg CO_2-equivalent per kilogram of IPA (Wernet et al., 2016), the biotechnological pathways for IPA synthesis demonstrate a clear environmental benefit. When compared to the market price of sugar at $0.5926 per kilogram (MacroTrends 2023), the selling price of IPA stands at $1.56 per kilogram, while its production costs range between $0.42 and $0.48 per kilogram. This suggests that the profit margin for IPA is nearly twice the market price of sugar. Given this significant price difference, converting sugar to IPA emerges as a cost-effective process. The findings suggest that bio-based IPA production, through optimized supply chain configurations, offers a more economical and sustainable alternative compared to conventional chemical synthesis processes. This is particularly significant in the context of stringent environmental regulations and a market increasingly sensitive to the carbon footprint of industrial activities.

3.2. Effects of scale-up on production cost and emission performance of the biorefinery plants

Fig. 6 shows the results of case (ii): optimal emissions performance (Fig. 6a) and production cost (Fig. 6b), respectively. The production costs exhibit a nearly linear increase with the increase in design capacity. However, at lower capacities (<300,000 mt/year), the cost performance demonstrates non-linear characteristics. This non-linearity arises from the strategic adaptations the system undergoes to expand in response to varying IPA demands (for a more detailed discussion, see Section 3.4). CO_2 emission performance illustrates a similar increasing linear trend as capacity increases. Nonetheless, as shown in Fig. 6a, a notable emission shift occurs in smaller capacity scenarios (below 37,200 mt/year). The observed shifted in emissions is primarily due to the scale-dependent emission factors incorporated into this study. A power law scaling factor (Caduff et al., 2014; Bahlawan et al., 2021) is utilized to quantify the impact of plant size on emissions demonstrating the variation of GWP100 with respect to the scale of IPA production. For large-scale operations, the GWP100 is determined to be 2.47 kg of CO_2-equivalent per kg of IPA. Conversely, small-scale operations experience a significantly increased GWP100 at 5.54 kg of CO_2-equivalent per kg of IPA, which is over twice the amount emitted by larger-scale plants. Meanwhile, the GWP100 for medium-sized IPA production processes is measured at 3.57 kg of CO_2-eq per kg of IPA. This marked disparity is highlighted in Fig. 6a (details in Fig. 10a, Section 3.4), where it becomes evident that smaller-scale bio-IPA plants experience proportionally greater emissions under the conditions analyzed.

The increasing trend as a function of capacity in both cost and emissions is influenced by transportation costs, which increase as the supply chain complexity increases. This complexity arises from the growing distance between facilities and an expansion in the number of sites, reaching a point where economies of scale for inbound transportation no longer apply (Minner, 2019). Typically, optimal site selection entails a balance between the number of facilities that minimize total logistics costs. There is an initial decrease in costs but beyond the optimal threshold costs begin to increase (Fig. 7). For instance, if the design supply chain wants to respond to the increasing demands of IPA, it may have to increase the number of facilities which is beyond the point that minimizes logistics costs.

As shown in Fig. 7, the scenarios that are optimized for cost highlight the significant impact of biomass expenses. The major expenditure, which accounts for almost 70 % of the total cost, is attributed to the procurement of raw materials, including biomass and for the sugar production processes. It is worth noting that the IPA production process is responsible for the largest share, approximately 50 %, of emissions in the bio-IPA production lifecycle. Additionally, the contribution of transportation to both cost and emissions increases with an increase in the annual production capacity of the design, emphasizing the importance of logistics in the operational design of the biorefinery.

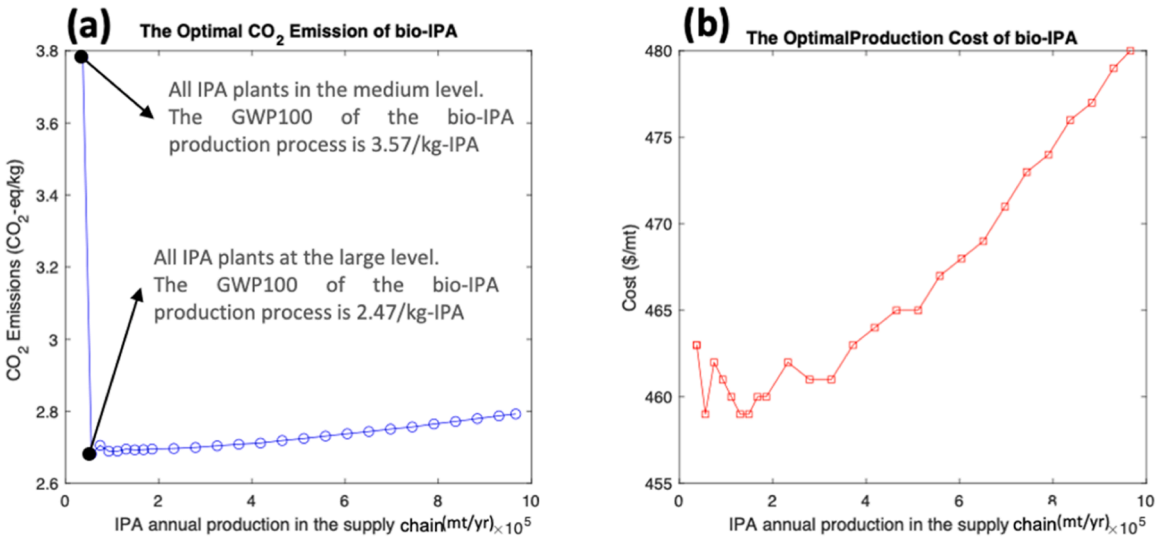

Fig. 6. Emissions and costs versus IPA production capacity. Fig. 6a shows CO_2 emissions per kg of IPA. The shift in emissions is driven by the variation in GWP100 of scale of IPA production, with a power law scaling factor applied to account for the scale differences. At a medium scale, the IPA production process results in a GWP100 of 3.57 kg of CO_2-equivalent per kg of IPA, while at a large scale, the GWP100 is reduced to 2.47 kg of CO_2-equivalent per kg of IPA. Fig. 6b illustrates rising production costs per metric ton as capacity scales up.

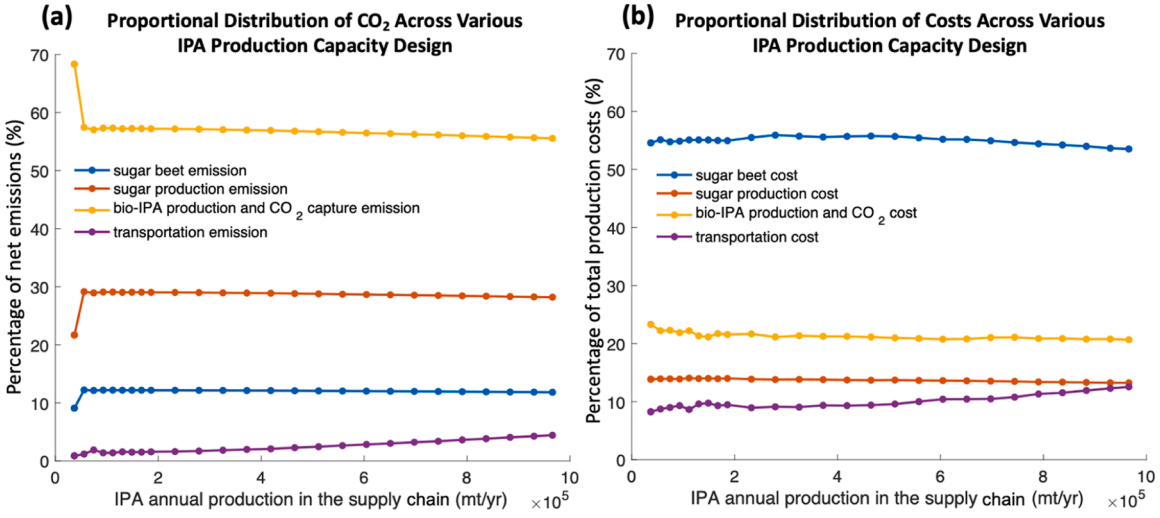

Fig. 7. Stacked proportional distribution of CO_2 emissions and costs in IPA production capacity designs. Fig. 7a shows emission contributions by sector for varying IPA production levels, while Fig. 7b shows the corresponding cost breakdown. Each color represents a different aspect of the supply chain, highlighting the emissions and costs associated with transportation, bio-IPA production, sugar processing, and sugar beet cultivation as IPA production scales.

3.3. Structural similarity in supply chain configurations for Bio-IPA production

The optimal supply chain configurations are different under varying objectives and production capacity. Here, the structural similarity is introduced to observe the configuration similarity between the economic and environmental performance objectives at the same IPA capacity level. In this study, we employ the Structural Similarity Index Measure (SSIM) as a metric to evaluate the structural similarity in supply chain networks (Wang et al., 2004), where the supply chain information is encoded as 2-dimensional matrices. For an example, the connectivity within the supply chain is encoded in a binary matrix, X, of dimensions 25×5, where the rows correspond to sugarbeet supply counties and the columns to sugar plants. An element $X_{ij} = 1$ indicates an active supply link between county i and sugar plant j. The SSIM index is represented by the Eq. (35), (Wang et al., 2004):

$$SSIM = \frac{\left(2\mu_x\mu_y + (k_1L)^2\right)\left(2\sigma_{xy} + (k_2L)^2\right)}{\left(\mu_x^2 + \mu_y^2 + (k_1L)^2\right)\left(\sigma_x^2 + \sigma_y^2 + (k_2L)^2\right)} \tag{35}$$

where μ_x and μ_y are the mean values of two-dimensional matrices that encode the configuration of the supply chain for the cost (X) and emission (Y) objectives, respectively. σ_x^2 and σ_y^2 are the variances of each matrix, σ_{xy} is the covariance for two supply chains, and k_1L and k_2L are constants to stabilize division with weak denominator, provides a comprehensive measure of similarity between two entities (Wang et al., 2003). Originally developed for image analysis, SSIM's application in this context offers an innovative approach to quantitatively compare the structures of supply chain networks, providing valuable insights into their organizational efficiency and robustness. In particular, the SSIM metric helps interpret how closely a given supply chain configuration aligns with an ideal or optimal structure under different considerations.

Fig. 8 shows the SSIM for supply chains under various capacities. Specifically, Fig. 8a illustrates the SSIM for the supply chain segment from the biomass farm to the sugar plant, while Fig. 8b focuses on the segment from the sugar plant to the IPA plant. The index indicates that supply chain configurations under environmental and economic objectives exhibit greater similarity as the annual IPA production increases. Specifically, the supply connections from sugar beet supply counties to sugar production plants align under both objectives when IPA production exceeds approximately 700,000 mt (SSIM index = 1). The connections between sugar plants and bio-IPA plants as shown in Fig. 8b using either objective show an increasing SSIM index with larger IPA production capacity, yet they do not converge into identical configurations.

Moreover, the SSIM index was utilized to select supply chain configurations under three distinct annual production capacities, illustrating structural differences between objectives. Fig. 9 displays the optimal supply chain configurations for IPA capacities of 186,000, 409,200, and 965,898 mt/year, optimized for cost and carbon dioxide emissions scenarios. These capacities were chosen based on their SSIM index ranges, which are indicative of structural similarity: low (0–0.3), medium (0.4–0.6), and high (0.8–1). At the capacity of 186,000 mt/year, in the case of optimized for CO_2 emission performance, the supply chain configurations tend to cluster in regions that facilitate a sequential supply chain from raw material sourcing to production, without overlapping sources. In contrast, for cost optimization scenarios, supply chain configurations are more spread out, making the selected bio-IPA plant farther away from the raw material sources than the CO_2 emission optimization scenarios. This difference highlights the significance of transportation emissions in minimization of emission objective, while in cost minimization objective, the raw material costs, particularly sugar beets, are more important contributor (the selected sugar beet farms are located at the largest sugar beet production counties with cheaper prices). As the target IPA production volume increases, the structures of the two configurations become more similar, owing to the system's need to meet the IPA demand, thereby limiting the flexibility in site selection.

3.4. Flow logistics analysis

In this section, an investigation into strategic adaptations in supply chain management in response to increasing demand is conducted, with a focus on the logistic flows within supply chains and the scaling of individual sites. Fig. 10 illustrates the optimal supply chain configurations under various IPA capacities. The analysis reveals three strategic phases in supply chain design to accommodate rising demand. Initially, an expansion in the scale of facilities, particularly sugar plants and IPA production plants, is observed. This expansion, following the 0.7 power law of scaling, leads to more efficient production costs and improved environmental performance. For instance, with the increase in demand of IPA from 232,500 mt/yr to 744,000 mt/yr, larger scale plants are noted, resulting in a reduction in sugar production unit cost from $107.51/mt to $102.96/mt and improved production emissions (as shown in Fig. 6a). Subsequently, the formation of additional clusters is identified as a key strategy, leading to improved transportation emissions. In supply chain configurations at a design capacity of 111,600 mt/yr, two clusters are evident in both scenarios. This clustering is shown to decrease the average unit transportation emissions from 0.06 CO_2-eq/kg-IPA to 0.05 CO_2-eq/kg-IPA when capacity increases from 74,400 mt/yr to 111,600 mt/yr.

The final phase is characterized by an increase in the number of facilities within these clusters, introducing more branches into the supply chain. As design capacity expands, an increase in facility count is noted. The increasing of branches within a cluster may result in worse transportation emission efficiency and transportation costs. When comparing supply chain configurations at 232,500 mt/yr and 325,500 mt/yr, while the number of clusters remains constant, an increase in the cluster size in southwest Minnesota is observed due to the addition of IPA biorefinery sites. This change leads to an increase in transportation routes from sugar plants to new biorefineries, raising the unit transportation emission from 0.05 CO_2-eq/kg-IPA to 0.06 CO_2-eq/kg-IPA. However, a marginal improvement in IPA production cost is observed, decreasing from $64.0/mt to $63.8/mt, attributable to the increased site capacity. Conversely, the transportation cost sees a slight increase, moving from $41.3/mt to $41.8/mt, as the new facilities are located further from the original supply chain design sites.

As a result, based on the strategies in response to the increasing demand discussed above, the scaling-up of plant capacities emerges as the most important strategy in dealing with increasing demand, offering benefits in both cost and emissions. However, as demand increases, the capacity limits and resource constraints at the county level may reach their upper bounds, making the original design infeasible. To

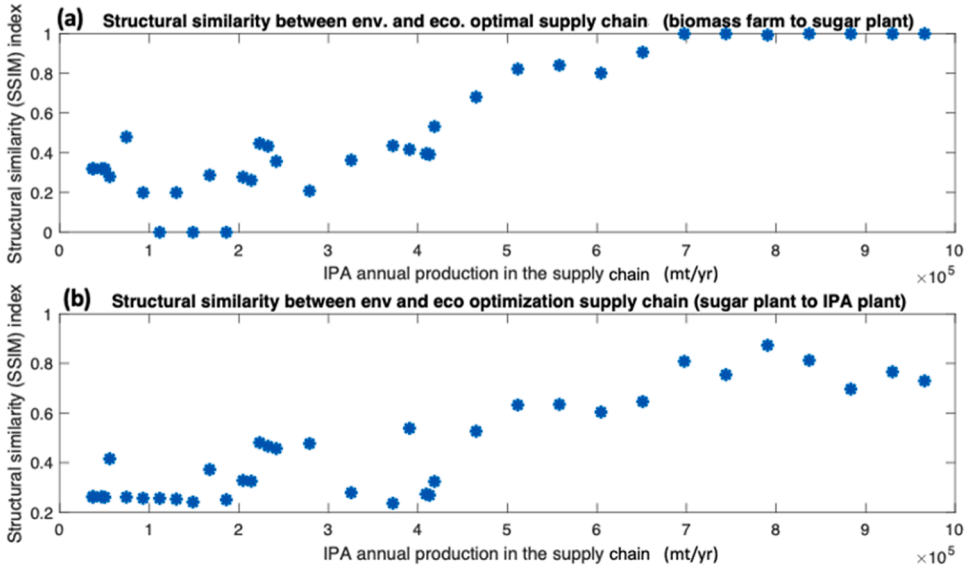

Fig. 8. Comparative analysis of structural similarity in supply chain configurations for economic and environmental objectives. This figure illustrates the supply chain configurations segmented into two distinct phases: from biomass farm to sugar plant (Fig. 8a), and from the sugar plant to the IPA plant (Fig. 8b). The analysis emphasizes the structural similarities and differences between the supply chain setups when tailored to meet either economic or environmental objectives.

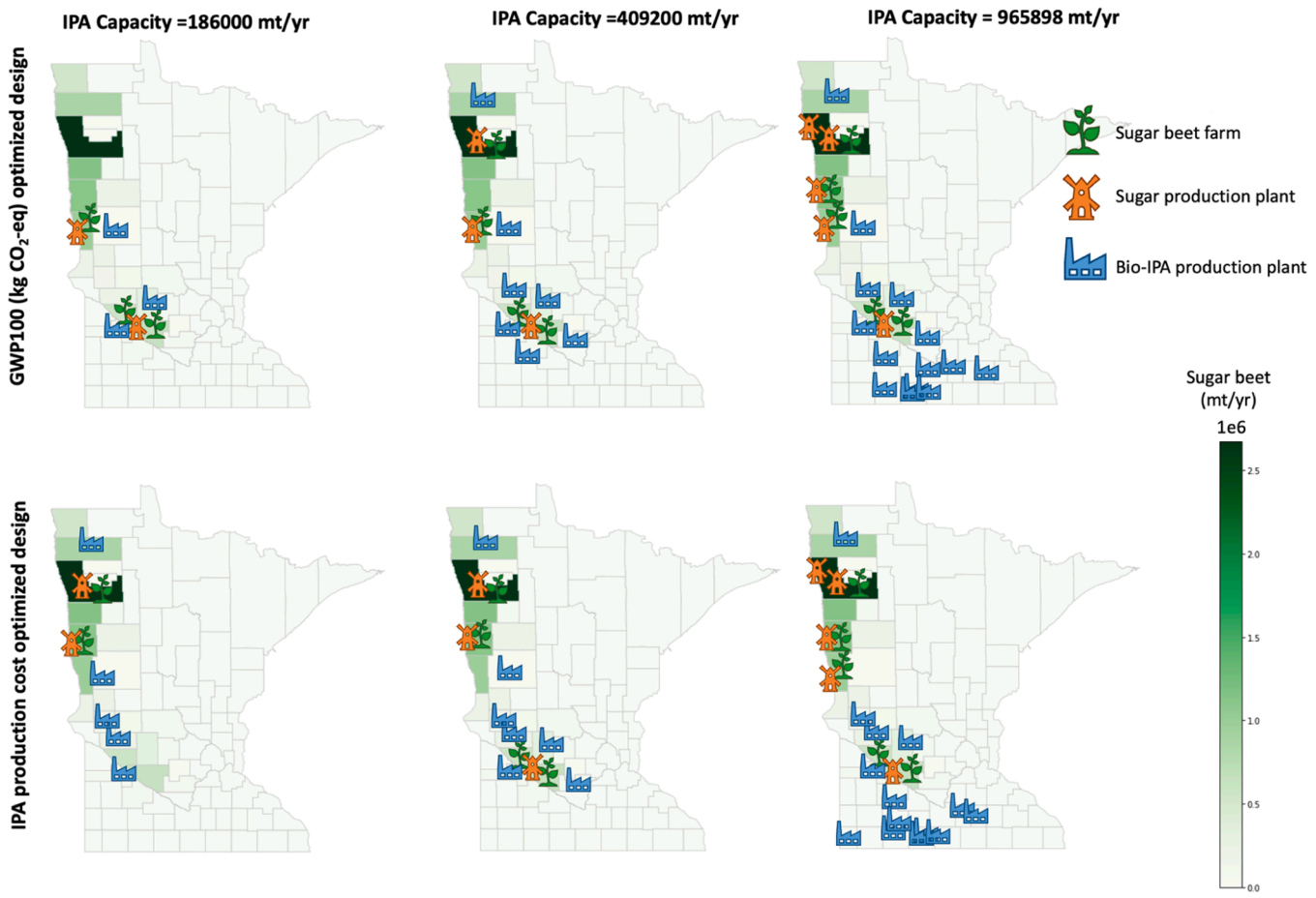

Fig. 9. The optimal supply chain configurations at different scenarios. The top panel illustrates the supply chains' GWP impact in terms of CO_2 equivalent emissions across three IPA production scenarios: 186,000 mt/yr, 409,200 mt/yr, and 965,898 mt/yr. The bottom panel displays the corresponding production costs. Icons represent sugar beet farms (green), sugar production plants (orange), and bio-IPA production plants (blue), with the scale for sugar beet throughput (mt/yr) shown on the gradient bar. The configurations reflect the strategic placement of operations to optimize either environmental impact or cost efficiency at different production scales.

accommodate this increased demand, the supply chain adapts by adding new facilities, often leading to the formation of new sugar beet-to-IPA plant clusters aiming at reducing the transportation costs. The three phases of industrial expansion in isopropanol (IPA) production explain the nonlinear oscillatory behavior, as depicted in Fig. 6b, within the capacity range of up to approximately 320,000 mt per year.

In this study, a maximum of three clusters of sugar beet-to-IPA supply chain are identified, each situated strategically across the state. The first cluster is located in the northwest, offering access to the most cost-effective sugar beet resources. The second cluster is in the central west of the state, advantageous due to the presence of two sugar plants that provide ample capacity for processing sugar beet to meet the raw material demand. The final cluster is located in the southwest of the state, distinguished by its potential for IPA production sites, offering ample CO_2 off-gas, which translates to more efficient transportation costs and emissions.

When the number of clusters reaches three, adding facilities in each cluster begins as demand continues to rise. While this expansion strategy is derived from our optimization analysis, it's important to note that it may not always result in enhanced performance regarding emission reduction and production costs. This observation suggests that the supply chain might have attained its peak efficiency in terms of inbound transportation economies. This conclusion is not merely empirical but is supported by the optimization models we employed, indicating a calculated point of diminishing returns in the supply chain's performance. At this point, the focus may shift to optimizing within these established clusters, seeking efficiencies in operations and logistics to maintain or improve the supply chain's overall effectiveness in the face of growing demand.

3.5. *Bio-Based isopropanol production: advancing towards sustainable chemical synthesis*

In sustainable chemical production, bio-based IPA is gaining traction due to its versatile applications and reduced environmental impact. Used as a solvent, antiseptic, and fuel additive, IPA's production from sugar beets exemplifies the transition to greener methodologies, potentially lowering the carbon footprint over traditional processes.

The competitiveness of IPA production from sugar beets can be effectively assessed by comparing its production costs and emissions with those from other biotechnological methods. The process of converting CO_2 and sugar into IPA via engineered autotrophic acetogens, such as *Clostridium autoethanogenum* (Liew et al., 2022; Bankar et al., 2015), as well as the utilization of industrial off-gas (steel mill off-gas) through gas fermentation, demonstrates potential for negative GHG emissions. Reported emissions for these innovative pathways are as low as -1.17 CO_2-eq/kg for IPA (Liew et al., 2022), highlighting a significant environmental advantage over conventional petrochemical synthesis, which has associated emissions of around 3.27 CO_2-eq/kg-IPA. In comparison, the bio-based approach for producing IPA from sugar beets has documented emissions of 2.68 CO_2-eq/kg-IPA. While this does not reach the negative emissions mark of gas fermentation, it is a marked

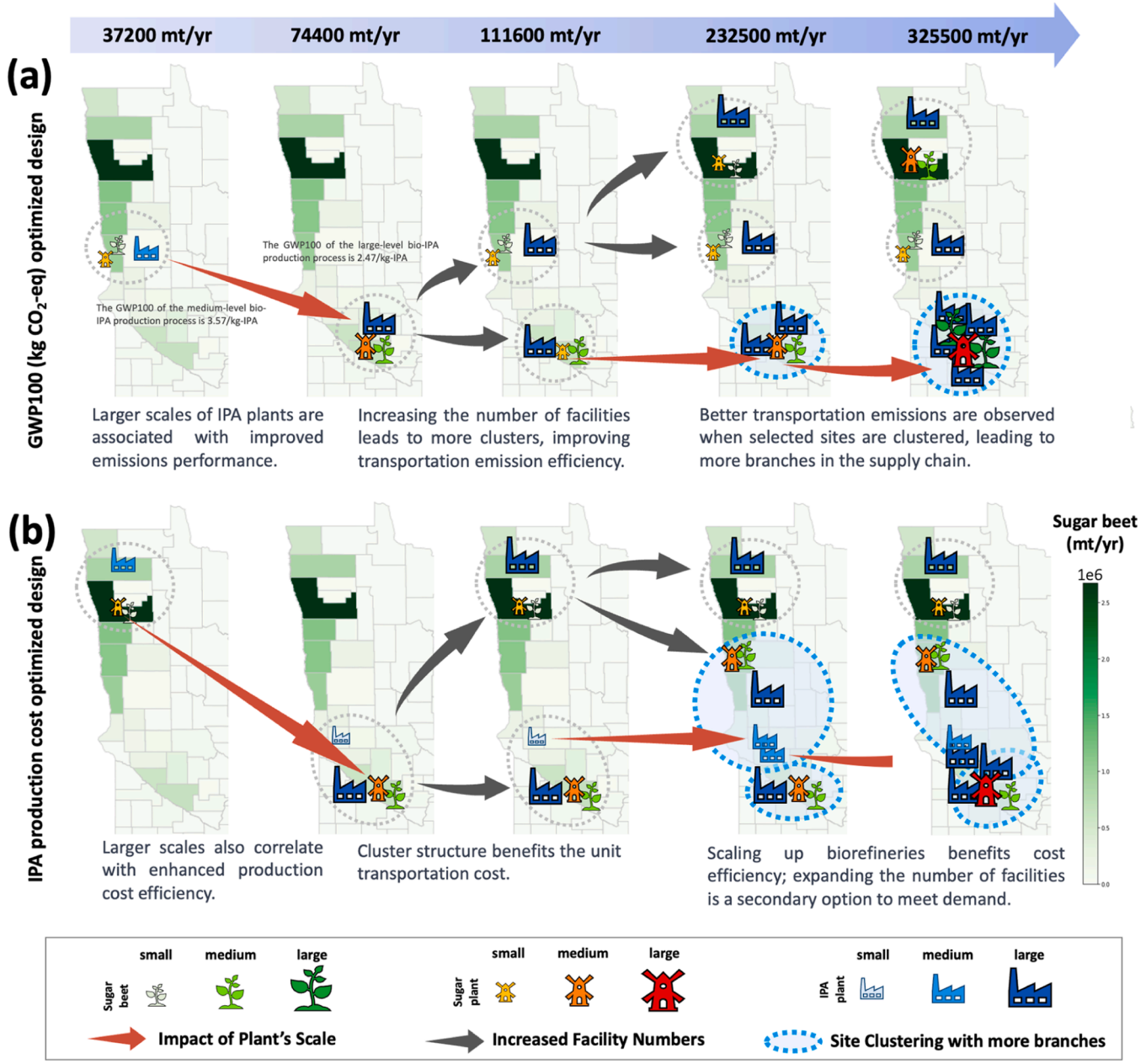

Fig. 10. Progressive Scaling and Clustering Strategies in Supply Chain Optimization for IPA Production. This figure maps out the adjustments in supply chain design with increasing IPA demand, showing transitions from enlarging plant scales to forming clusters and expanding facility numbers. It contrasts the supply chain configurations under environmental impact (Fig. 10a) with those under cost efficiency (Fig. 10b) as annual demand grows from 37,200 mt/yr to 325,500 mt/yr. The size of facilities (small, medium, large) and the extent of clustering are visualized at different demand levels, indicating the strategic shift from scaling individual plants to creating more extensive supply chain networks with additional branches for enhanced efficiency and lower emissions.

reduction from the emissions of traditional petrochemical methods. The primary distinction lies in the innovative use of CO_2 as a feedstock, contributing to a reduced carbon footprint. These findings suggest that bio-based IPA from sugar beets is a viable and more sustainable alternative in the chemicals market, aligning with global efforts to mitigate climate change through carbon-conscious industrial practices.

3.6. Computational details

All computations were performed using GAMS® software on an Intel Core i7–11850H CPU @ 2.50 GHz processor with 64.0 GB RAM. Solving the MILP required few seconds, demonstrating the computational advantage of the piecewise linearization method for sugar and IPA production costs. There are 312 single equations and 407 single variables in the model. The overall procedure lasted: (i) MILP: a few seconds (1–2 s) to find the maximum and minimum s, respectively; (ii) MILP: up to approximately 0.3 s to identify the optimal supply chain configuration for economic and CO_2 emissions scenarios, respectively; and (iii) MILP: about 1∼2 min to solve the Pareto solution sets with ϵ-constraint method. The computational time linearly increases with more Pareto solution sets solved for varying IPA demand scenarios.

4. Conclusions

The GIS-enabled supply chain optimization model introduced in this study for the Sugar Beet-to-Isopropanol (bio-IPA) production in Minnesota aimed to minimize annual production costs and environmental impacts. It achieved this by optimizing the numbers, locations, and

capacities of farms, processing facilities, and biorefineries, as well as identifying the most efficient biomass flow patterns. The utilization of GIS was crucial for generating spatial data related to biomass production and determining the shortest transportation routes using the existing road and railway networks. The results from the baseline scenario, considering the increasing demand for bio-IPA, showed that economies of scale could be realized, with unit production costs reaching their minimum at a production capacity of 55,800 mt/year. At this scale, significant cost and emission reductions were apparent, highlighting the strategic balance between scale expansion and logistical efficiency.

The study revealed that supply chain configurations are highly responsive to changes in IPA demand. The strategic scaling up of facilities and the clustering of operations emerged as key responses to increasing demand, with both measures leading to reduced transportation emissions and costs. However, the production costs and emissions performance are not always directly scalable. As the study suggests, while larger scales typically yield more cost-efficient operations due to economies of scale, there are practical limits to these benefits (Malmberg and Maskell, 1997). When the demand scale is between 37,200 to 325,500 mt/yr, finite resources and the capacity constraints of plants introduce a complexity where production costs and LCA emissions performance do not linearly align with scale increases. This suggests that beyond a certain point, that is demand scale exceeds 325,500 mt/yr, the benefits of scaling diminish, and further expansion could lead to increased production emissions and costs due to less efficient transportation logistics.

In conclusion, this research provides a detailed approach for optimizing sustainable supply chains in the bio-based chemical industry. It showcases the importance of strategic planning and logistical efficiency in achieving both economic and environmental objectives. The study affirms the economic and environmental advantages of bio-IPA production, highlighting its potential profitability and lower emission profile compared to conventional chemical synthesis processes. The findings are significant for the development of sustainable industrial practices, demonstrating that with appropriate optimization strategies, bio-based chemical production can be economically viable and environmentally sustainable, even as it scales up to meet increasing demand and complies with rigorous environmental regulations. The model introduced in the study serves as a foundational blueprint for bio-IPA plant development planning. However, for enhanced precision, incorporating more accurate distance calculations that factor in road and rail logistics across a broader supply chain could yield more reliable estimates of emissions and economic outcomes. Additionally, identifying and addressing potential risks, such as supplier failures, logistics disruptions, or market changes (e.g., reallocating the sugar that would have been exported to other countries to isopropanol production), allows for more informed strategic decision-making, such as selecting warehouse locations or supplier partnerships. These areas of investigation hold substantial potential for future scholarly and practical advancements.

CRediT authorship contribution statement

Ching-Mei Wen: Writing – original draft, Resources, Methodology. **Marianthi Ierapetritou:** Writing – review & editing, Supervision, Conceptualization.

Declaration of competing interest

The authors declare that they have no known competing financial interests or personal relationships that could have appeared to influence the work reported in this paper.

Data availability

Data will be made available on request.

Acknowledgments

This work was supported by a US Department of Energy ARPA-E program DE-FOA-0002387, NSF program 2217472 and NSF 2134471.

Supplementary materials

Supplementary material associated with this article can be found, in the online version, at doi:10.1016/j.compchemeng.2024.108836.

References

Allen, M.R., Fuglestvedt, J.S., Shine, K.P., Reisinger, A., Pierrehumbert, R.T., Forster, P. M, 2016. New use of global warming potentials to compare cumulative and short-lived climate pollutants. Nat. Clim. Chang. 6 (8), 773–776.

Allman, A., Daoutidis, P., Tiffany, D., Kelley, S., 2017. A framework for ammonia supply chain optimization incorporating conventional and renewable generation. AIChE Journal 63 (10), 4390–4402.

American Chemistry, C. Statista. 2020. U.S. isopropanol production volume. Assessed: Dec 11 2023. from https://www.statista.com/statistics/974791/us-isopropanol-production-volume.

An, H., Wilhelm, W.E., Searcy, S.W., 2011. A mathematical model to design a lignocellulosic biofuel supply chain system with a case study based on a region in Central Texas. Bioresour. Technol. 102 (17), 7860–7870.

Anand, R., Aggarwal, D., Kumar, V., 2017. A comparative analysis of optimization solvers. J. Statistic. Manag. Syst. 20 (4), 623–635.

Bahlawan, H., Morini, M., Spina, P.R., Venturini, M., 2021. Inventory scaling, life cycle impact assessment and design optimization of distributed energy plants. Appl. Energy 304, 117701. https://doi.org/10.1016/j.apenergy.2021.117701 (acccessed 2023/12/12/04:21:55)From DOI.org (Crossref).

Bangsund, D.A.; Leistritz, F.L.; Bangsund, D.A.; Leistritz, F.L. Economic contribution of the sugarbeet industry in Minnesota, North Dakota and eastern Minnesota. 2004. DOI: 10.22004/AG.ECON.23618 (acccessed 2023/12/11/22:06:57). From DOI.org (Datacite).

Bankar, S.B., Jurgens, G., Survase, S.A., Ojamo, H., Granström, T., 2015. Genetic engineering of Clostridium acetobutylicum to enhance isopropanol-butanol-ethanol production with an integrated DNA-technology approach. Renew. Energy 83, 1076–1083. https://doi.org/10.1016/j.renene.2015.05.052 (acccessed 2023-01-30 14:57:14)DOI.org (Crossref).

Beef2Live. (n.d.). Ranking Of States That Produce Sugarbeets. Accessed: Nov 6 2023, from https://beef2live.com/story-ranking-states-produce-sugarbeets-0-212386.

Boisvert, R.F., Howe, S.E., Kahaner, D.K., 1985. GAMS: a framework for the management of scientific software. ACM Trans. Math. Softw. 11 (4), 313–355. https://doi.org/10.1145/6187.6188 (acccessed 2023/12/11/22:25:43)From DOI.org (Crossref.

Borghesi, G., Stefanini, R., Vignali, G., 2022. Life cycle assessment of packaged organic dairy product: a comparison of different methods for the environmental assessment of alternative scenarios. J. Food Eng. 318, 110902 https://doi.org/10.1016/j.jfoodeng.2021.110902 (acccessed 2023/01/15/08:19:03)From DOI.org (Crossref.

Burrough, P.A.; McDonnell, R.A.; Lloyd, C.D. *Principles of Geographical Information Systems*; Oxford University Press, 2015.

Caduff, M., Huijbregts, M.A.J., Koehler, A., Althaus, H.J., Hellweg, S., 2014. Scaling Relationships in Life Cycle Assessment: the Case of Heat Production from Biomass and Heat Pumps. J. Ind. Ecol. 18 (3), 393–406. https://doi.org/10.1111/jiec.12122 (acccessed 2023/12/12/04:08:27)From DOI.org (Crossref.

Campbell, L.G., 2002. Sugar beet quality improvement. J. Crop. Prod. 5 (1–2), 395–413.

Charubin, K., Papoutsakis, E.T., 2019. Direct cell-to-cell exchange of matter in a synthetic Clostridium syntrophy enables CO2 fixation, superior metabolite yields, and an expanded metabolic space. Metab. Eng. 52, 9–19. https://doi.org/10.1016/j.ymben.2018.10.006 (acccessed 2022/02/09/01:46:08)From DOI.org (Crossref.

ChemAnalyst. (2023). Isopropyl alcohol - price & market analysis. Accessed: Nov 1 2023, from https://www.chemanalyst.com/Pricing-data/isopropyl-alcohol-31.

Cheng, M.H., Huang, H., Dien, B.S., Singh, V., 2019. The costs of sugar production from different feedstocks and processing technologies. Biofuels, Bioprod. Biorefining 13 (3), 723–739. https://doi.org/10.1002/bbb.1976 (acccessed 2023/01/15/07:46:34) From DOI.org (Crossref.

Cherubini, F., Guest, G., Strømman, A.H., 2012. Application of probability distributions to the modeling of biogenic CO2fluxes in life cycle assessment. GCB Bioenergy 4 (6), 784–798. https://doi.org/10.1111/j.1757-1707.2011.01156.x.

Chung, W., Jeong, W., Lee, J., Kim, J., Roh, K., Lee, J.H., 2023. Electrification of CO2 conversion into chemicals and fuels: gaps and opportunities in process systems engineering. Comput. Chem. Eng. 170.

De Jong, E., Higson, A., Walsh, P., Wellisch, M., 2012. Product developments in the bio-based chemicals arena. Biofuels Bioproduct. Biorefin. 6 (6), 606–624. https://doi.org/10.1002/bbb.1360 (acccessed 2023/12/11/22:48:44)From DOI.org (Crossref.

Duraisam, R., Salelgn, K., Berekete, A.K., 2017. Production of beet sugar and bio-ethanol from Sugar beet and it bagasse: a Review. IJETT 43 (4), 222–233. https://doi.org/10.14445/22315381/IJETT-V43P237 (acccessed 2023/12/11/21:59:25)From DOI.org (Crossref.

Eggleston, G., Lima, I., 2015. Sustainability Issues and Opportunities in the Sugar and Sugar-Bioproduct Industries. Sustainability. 7 (9), 12209–12235. https://doi.org/10.3390/su70912209 (acccessed 2023/12/11/21:57:01)From DOI.org (Crossref).

Fenila, F., Shastri, Y., 2020. Stochastic optimization of enzymatic hydrolysis of lignocellulosic biomass. Comput/ Chem. Eng. 135, 685–695. Athaley, A.; Annam, P.; Saha, B.; Ierapetritou, M. Techno-economic and life cycle analysis of different types of hydrolysis process for the production of p-Xylene. *Computers & Chemical Engineering* **2019**, *121*.

Fiorentino, G., Zucaro, A., Ulgiati, S., 2019. Towards an energy efficient chemistry. Switching from fossil to bio-based products in a life cycle perspective. Energy 170, 720–729. https://doi.org/10.1016/j.energy.2018.12.206 (acccessed 2023/12/11/ 21:42:34)From DOI.org (Crossref).

Foster, C., Charubin, K., Papoutsakis, E.T., Maranas, C.D., 2021. Modeling growth kinetics, interspecies cell fusion, and metabolism of a clostridium acetobutylicum/ Clostridium ljungdahlii Syntrophic Coculture. mSystems. 6 (1), e01325. https://doi.org/10.1128/mSystems.01325-20. -01320(acccessed 2023/01/30/15:30:37)From DOI.org (Crossref.

Gavrilescu, M., Chisti, Y., 2005. Biotechnology—A sustainable alternative for chemical industry. Biotechnol. Adv. 23 (7–8), 471–499. https://doi.org/10.1016/j.biotechadv.2005.03.004 (acccessed 2023/12/11/21:47:24)From DOI.org (Crossref.

Ghafoori, E., Flynn, P., Feddes, J., 2007. Pipeline vs. truck transport of beef cattle manure. Biomass and Bioenergy 31 (2–3), 168–175. https://doi.org/10.1016/j.biombioe.2006.07.007 (acccessed 2023/12/11/23:48:15)From DOI.org (Crossref.

Global chemical industry. (n.d.), E. c. p. *global chemical industry B2B website*. https://www.echemi.com (accessed 2023 Nov 6).

Google, I. *Google maps distance matrix API*; 2017.

Gray, P., 1971. Exact solution of the fixed-charge transportation problem. Oper. Res. 19 (6), 1529–1538.

Jafari-Nodoushan, A., Sadrabadi, M.H.D., Nili, M., Makui, A., Ghousi, R., 2024. Designing a sustainable disruption-oriented supply chain under joint pricing and resiliency considerations: a case study. Comput. Chem. Eng. 180.

Kádár, Z.; Fonseca, C. Bio-products from sugar-based fermentation processes. In *Biorefinery*, Bastidas-Oyanedel, J.R., Schmidt, J. E. Eds.; Springer International Publishing, 2019; pp 281–312.

Kahn, T., Bosch, J., Levitt, M.F., Goldstein, M.H., 1975. Effect of sodium nitrate loading on electrolyte transport by the renal tubule. Am. J. Physiol. 229 (3), 746–753. https://doi.org/10.1152/ajplegacy.1975.229.3.746. From PubMed.

Kropf, H., 1966. Alcohols as petrochemicals. Angewandte Chemie Int. Edit. English 5 (7), 646–653.

L, Z.OPENCAGEGEO: Stata module for forward and reverse geocoding using the OpenCage Geocoder API Stat Softw Components. 2016.

Lee, J., Jang, Y.-S., Choi, S.J., Im, J.A., Song, H., Cho, J.H., Seung, D.Y., Papoutsakis, E. T., Bennett, G.N., Lee, S.Y., 2012. Metabolic engineering of clostridium acetobutylicum ATCC 824 for isopropanol-butanol-ethanol fermentation. Appl. Environ. Microbiol. 78 (5), 1416–1423. https://doi.org/10.1128/AEM.06382-11 (acccessed 2022/07/18/15:48:49)From DOI.org (Crossref).

Lee, R.A., Lavoie, J.M., 2013. From first- to third-generation biofuels: challenges of producing a commodity from a biomass of increasing complexity. Anim. Front. 3 (2), 6–11. https://doi.org/10.2527/af.2013-0010 (acccessed 2023/12/11/21:53:03) From DOI.org (Crossref.

Lewis, M.U.S. Department of energy announces selection of seven clean hydrogen hubs. https://www.morganlewis.com/blogs/powerandpipes/2023/11/us-department-of-energy-announces-selection-of-seven-clean-hydrogen-hubs. accessed Jan 5 2024.

Liebeck, T.; Meyer, T.; Abele, E. Production technology: adapting to maximize local advantage. In *Global Production*, Abele, E., Meyer, T., Näher, U., Strube, G., Sykes, R. Eds.; Springer Berlin Heidelberg, 2008; pp 192–235.

Liew, F.E., Nogle, R., Abdalla, T., Rasor, B.J., Canter, C., Jensen, R.O., Wang, L., Strutz, J., Chirania, P., De Tissera, S., et al., 2022b. Carbon-negative production of acetone and isopropanol by gas fermentation at industrial pilot scale. Nat. Biotechnol. 40 (3), 335–344. https://doi.org/10.1038/s41587-021-01195-w (acccessed 2022-04-08 03:58:59)DOI.org (Crossref).

Liew, F.E., Nogle, R., Abdalla, T., Rasor, B.J., Canter, C., Jensen, R.O., Wang, L., Strutz, J., Chirania, P., De Tissera, S., et al., 2022a. Carbon-negative production of acetone and isopropanol by gas fermentation at industrial pilot scale. Nat. Biotechnol. 40 (3), 335–344. https://doi.org/10.1038/s41587-021-01195-w. From NLM Medline.

Lim, J.S., Benjamin, M.F.D., Van Fan, Y., You, F., 2023. Approaches towards a sustainable and low carbon emissions production. J. Clean. Prod.

Lin, T., Rodríguez, L.F., Shastri, Y.N., Hansen, A.C., Ting, K., 2013. GIS-enabled biomass-ethanol supply chain optimization: model development and Miscanthus application. Biofuels, Bioproduct. Biorefin. 7 (3), 314–333. https://doi.org/10.1002/bbb.1394 (acccessed 2023/12/ 12/04:31:56)From DOI.org (Crossref).

Lopes, M.S.G., 2015. Engineering biological systems toward a sustainable bioeconomy. J. Ind. Microbiol. Biotechnol. 42 (6), 813–838. https://doi.org/10.1007/s10295-015-1606-9 (acccessed 2023/12/11/21:50:09)From DOI.org (Crossref.

Lopes, T.C.; Brauner, N.; Magatão, L. Optimally solving multi-objective MILP problems with part-wise continuous Pareto fronts. In ROADEF 2020-21ème Congrès de la Société Française de Recherche Opérationnelle et D'aide à la Décision, 2020.

Ma, S., Shang, X., Zhu, M., Li, J., Sun, L., 2019. Design, optimization and control of extractive distillation for the separation of isopropanol-water using ionic liquids. Sep. Purif. Technol. 209, 833–850. https://doi.org/10.1016/j.seppur.2018.09.021 (acccessed 2023/12/11/23:10:27)From DOI.org (Crossref.

MacroTrends. (2023). Sugar prices - historical chart data. Accessed: Nov 17 2023, from https://www.macrotrends.net/2537/sugar-prices-historical-chart-data; (accessed.

Malmberg, A., Maskell, P., 1997. Towards an explanation of regional specialization and industry agglomeration. Eur. Plan. Stud. 5 (1), 25–41. https://doi.org/10.1080/09654319708720382 (acccessed 2023/12/12/05:09:29)From DOI.org (Crossref.

McPherson, B. *Integrated Mid-Continent Carbon Capture, Sequestration & Enhanced Oil Recovery Project*; Univ. of Utah, Salt Lake City, UT (United States). 2010.

Minner, S. Inbound logistics. In *Operations, Logistics and Supply Chain Management*, Zijm, H., Klumpp, M., Regattieri, A., Heragu, S. Eds.; Springer International Publishing, 2019; pp 233–249.

Minnesota Bio-Fuels Association. 2021. *Bioenergy Production Based On an Engineered Mixotrophic Consortium for Enhanced CO2 Fixation*. Advanced Research Projects Agency - Energy (ARPA-E). https://arpa-e.energy.gov/technologies/projects/bioenergy-production-based-engineered-mixotrophic-consortium-enhanced-co2 (accessed 2023).

Minnesota Bio-Fuels Association. (n.d.). Production in Minnesota. Accessed Oct 10 2023, from https://www.mnbiofuels.org/resources/production-in-minnesota.

Miret, C., Chazara, P., Montastruc, L., Negny, S., Domenech, S., 2016. Design of bioethanol green supply chain: comparison between first and second generation biomass concerning economic, environmental and social criteria. Comput. Chem. Eng. 85, 16–35.

Mohanty, A.K., Misra, M., Drzal, L.T., 2002. Sustainable bio-composites from renewable resources: opportunities and challenges in the green materials world. J. Polym. Environ. 10 (1/2), 19–26. https://doi.org/10.1023/A:1021013921916 (acccessed 2023/12/11/21:43:46)From DOI.org (Crossref.

Moon, H.G., Jang, Y.-S., Cho, C., Lee, J., Binkley, R., Lee, S.Y., 2016. One hundred years of clostridial butanol fermentation. FEMS Microbiol. Lett. https://doi.org/10.1093/femsle/fnw001 fnw001. https://biorxiv.org/lookup (acccessed 2023/12/11/22:56:48)From DOI.org (Crossref)Kumar, K.; Jadhav, S. M.; Moholkar, V. S. *Acetone-Butanol-Ethanol (ABE) fermentation with Clostridial Co-cultures for Enhanced Biobutanol Production*; Microbiology, 2023. doi/10.1101/2023.12.08.570763 (accessed 2023/ 12/11/22:57:22).

Mutel, C., 2017. Brightway: an open source framework for life cycle assessment. JOSS 2 (12), 236. https://doi.org/10.21105/joss.00236 (acccessed 2023/01/15/08:44:37) From DOI.org (Crossref.

Ng, R.T., Maravelias, C.T., 2016. Design of cellulosic ethanol supply chains with regional depots. Ind/ Eng. Chem. Res. 55, 3420–3432.

O'Neill, E.G., Martinez-Feria, R., Basso, B., Maravelias, C.T., 2022. Integrated spatially explicit landscape and cellulosic biofuel supply chain optimization under biomass yield uncertainty. Comput. Chem. Eng. 160 (107724).

Osman, A.I., Qasim, U., Jamil, F., Al-Muhtaseb, A.a.H., Jrai, A.A., Al-Riyami, M., Al-Maawali, S., Al-Haj, L., Al-Hinai, A., Al-Abri, M., et al., 2021. Bioethanol and biodiesel: bibliometric mapping, policies and future needs. Renew. Sustain. Energy Rev. 152, 111677 https://doi.org/10.1016/j.rser.2021.111677 (acccessed 2023/12/ 11/21:54:52). From DOI.org (Crossref). Jonker, J. G. G.; Junginger, M.; Posada, J.; Ioiart, C. S.; Faaij, A. P. C.; Van Der Hilst, F. Economic performance and GHG emission intensity of sugarcane- and eucalyptus-derived biofuels and biobased chemicals in Brazil. *Biofuels, Bioproducts and Biorefining* **2019**, *13* (4), 950-977. DOI: 10.1002/bbb.1986 (acccessed 2023/12/11/21:55:27). From DOI.org (Crossref).

Pappas, I., Avraamidou, S., Katz, J., Burnak, B., Beykal, B., Türkay, M., Pistikopoulos, E. N., 2021. Multiobjective optimization of mixed-integer linear programming problems: a multiparametric optimization approach. Ind. Eng. Chem. Res. 60 (23), 8493–8503.

Perez, H.D., Wassick, J.M., Grossmann, I.E., 2022. A digital twin framework for online optimization of supply chain business processes. Comput. Chem. Eng. 166.

Sharma, B., Ingalls, R.G., Jones, C.L., Khanchi, A., 2013. Biomass supply chain design and analysis: basis, overview, modeling, challenges, and future. Renew. Sustain. Energy Rev. 24, 608–627.

Shield, I. Sugar and starch crop supply chains. In *Biomass Supply Chains for Bioenergy and Biorefining*, Elsevier, 2016; pp 249–269.

States Department of Agriculture, National agricultural statistics service. (n.d.). [Title or Description of the Data]. Access: Oct 20 2023, from https://quickstats.nass.usda.gov/#4F24466B-B129-3370-B998-A912B22974C6.

Swidah, R., Wang, H., Reid, P.J., Ahmed, H.Z., Pisanelli, A.M., Persaud, K.C., Grant, C. M., Ashe, M.P., 2015. Butanol production in S. cerevisiae via a synthetic ABE pathway is enhanced by specific metabolic engineering and butanol resistance. Biotechnol. Biofuels 8 (1), 97. https://doi.org/10.1186/s13068-015-0281-4 (acccessed 2023/12/11/22:05:42From DOI.org (Crossref.

Townsend, C.O. *The Beet-Sugar Industry in the United States (No. 721)*; US Department of Agriculture, 1918.

Turchi, C.S.; Gage, S.; Martinek, J.; Jape, S.; Armijo, K.; Coventry, J.; Pye, J.; Asselineau, C.-A.; Venn, F.; Logie, W. *CSP Gen3: Liquid-Phase Pathway to SunShot*; National Renewable Energy Lab.(NREL), Golden, CO (United States); Sandia …, 2021.

Wang, J., Yin, Y., 2021. Clostridium species for fermentative hydrogen production: an overview. Int. J. Hydrogen. Energy 46 (70), 34599–34625. https://doi.org/10.1016/j.ijhydene.2021.08.052 (acccessed 2023/12/11/23:45:36)From DOI.org (Crossref.

Wang, Z., Bovik, A.C., Sheikh, H.R., Simoncelli, E.P., 2004. Image quality assessment: from error visibility to structural similarity. IEEE Trans. Image Process. 13 (4), 600–612. https://doi.org/10.1109/TIP.2003.819861 (acccessed 2023/12/12/04: 42:12)From DOI.org (Crossref.

Wang, Z.; Simoncelli, E.P.; Bovik, A.C. Multiscale structural similarity for image quality assessment. In The Thrity-Seventh Asilomar Conference on Signals, Systems & Computers, Pacific Grove, CA, USA; 2003.

Wernet, G., Bauer, C., Steubing, B., Reinhard, J., Moreno-Ruiz, E., Weidema, B., 2016. The ecoinvent database version 3 (part I): overview and methodology. Int J. Life Cycle Assess. 21 (9), 1218–1230. https://doi.org/10.1007/s11367-016-1087-8 (acccessed 2022/04/18/19:39:01)From DOI.org (Crossref.

Wyman, C.E., Goodman, B.J., 1993. Biotechnology for production of fuels, chemicals, and materials from biomass. Appl. Biochem. Biotechnol. 39-40 (1), 41–59. https://doi.org/10.1007/BF02918976 (acccessed 2023/12/11/21:48:38)From DOI.org (Crossref.

You, F., Tao, L., Graziano, D.J., Snyder, S.W., 2012. Optimal design of sustainable cellulosic biofuel supply chains: multiobjective optimization coupled with life cycle assessment and input-output analysis. AIChE J. 58, 1157–1180.
Yue, D., You, F., Snyder, S., 2014. Biomass-to-bioenergy and biofuel supply chain optimization: overview, key issues and challenges. Comput. Chem. Eng. 66, 36–56.
Zhang, F., Rodriguez, S., Keasling, J.D., 2011. Metabolic engineering of microbial pathways for advanced biofuels production. Curr. Opin. Biotechnol. 22 (6), 775–783. https://doi.org/10.1016/j.copbio.2011.04.024 (acccessed 2023/12/11/22:05:04) From DOI.org (Crossref.